SUPPLEMENTAL MATERIAL

Protein aggregation is an early manifestation of phospholamban p.(Arg14del)-related cardiomyopathy

Tim R. Eijgenraam, MSc[1]; Cornelis J. Boogerd, PhD[2]; Nienke M. Stege, MSc[1]; Vivian Oliveira Nunes Teixeira, PhD[1]; Martin M. Dokter, BASc[1]; Lukas E. Schmidt, MSc[3]; Xiaoke Yin, PhD[3]; Konstantinos Theofilatos, PhD[3]; Manuel Mayr, MD, PhD[3]; Peter van der Meer, MD, PhD[1]; Eva van Rooij, PhD;[2] Jolanda van der Velden, PhD[4]; Herman H.W. Silljé, PhD[1]; Rudolf A. de Boer, MD, PhD[1*]

[1]Department of Cardiology, University of Groningen, University Medical Center Groningen, Groningen, the Netherlands

[2]Hubrecht Institute, Royal Netherlands Academy of Arts and Sciences (KNAW), University Medical Center Utrecht, Utrecht, the Netherlands

[3]King's British Heart Foundation Centre, King's College London, London, United Kingdom

[4]Department of Physiology, Vrije Universiteit, Amsterdam University Medical Center, Amsterdam Cardiovascular Sciences, Amsterdam, the Netherlands

*Corresponding author

Supplemental Methods

Supplemental Figures

Supplemental Tables

Supplemental Methods

Animals

Generation and characterization of mice carrying the phospholamban (PLN) p.(Arg14del) pathogenic variant (R14del) has been described before.[8] In summary, a C57Bl6/N mouse line was generated, in which the third exon of the murine *Pln* gene, which contains the coding region for the PLN protein, was flanked by *loxP* sites (*floxed*) and followed by a third exon of the murine *Pln* gene with the c.40_42delAGA pathogenic variant (performed by PolyGene, Switzerland). To delete the *floxed* region, these mice were bred with mice expressing the *Cre* enzyme in the germline under the control of the hypoxanthine-guanine phosphoribosyltransferase (*Hprt*) promoter enhancer, replacing the murine wild-type (WT) *Pln* exon-3 with the murine R14del *Pln* exon-3 in the resulting offspring (PLN-R14$^{\Delta/+}$). The offspring was backcrossed into a C57Bl6/J background. Mice were housed per nest and per sex on a 12 h light / 12 h dark cycle with *ad libitum* access to chow and water. Cardiac analyses and euthanasia were performed under continuous anesthesia of 2% isoflurane (TEVA Pharmachemie, the Netherlands) mixed with oxygen, administered via an aerial dispenser. Heart and respiration rates and body temperature were continuously monitored throughout all procedures. Since we had no prior evidence for sex differences, both male and female mice were used as indicated per experiment. All data acquisition and analyses were performed in a blinded fashion.

Cardiac tissue samples of mice that underwent myocardial ischemia-reperfusion (I/R), myocardial infarction (MI) or corresponding sham surgery (remote of the infarcted area) were derived from a previously published study.[10] In summary, male 10- to 12-week-old C57Bl6/J mice were randomized to I/R, MI or sham surgery based on their body weights. Surgical procedures were preceded by a subcutaneous injection of 5.0 mg/kg carprofen (Rimadyl) for analgesic purposes. Mice were anesthetized, intubated and placed supine on a heating pad for mechanical ventilation. The left anterior descending (LAD) coronary artery was ligated permanently (MI) or temporarily for 60 min (I/R). The same procedure but without coronary ligation was performed as sham surgery. Eight weeks after MI surgery, left ventricular (LV)

function was assessed using cardiac magnetic resonance imaging (MRI). Following MRI measurements, mice were sacrificed and tissues were collected for further analyses. Mice that had myocardial I/R injury were sacrificed 3 days after surgery. Sham controls were sacrificed at the same age as the operated mice, and combined into a single control group.

Genotyping

For genotyping of PLN-R14del mice, DNA was isolated from ear cuts using the prepGEM Universal kit (ZyGEM Corporation, New-Zealand) following manufacturer's instructions for DNA isolation from solid tissue. Ear cuts were incubated with ORANGE+ buffer, Histosolv and prepGEM in demiwater at 52°C for 5 min, 75°C for 10 min and 95°C for 3 min using a T100 thermal cycler (Bio-Rad, CA, USA) to extract DNA. To identify genotypes, quantitative polymerase chain reaction (qPCR) analysis was performed using iQ SYBR green supermix (Bio-Rad) according to the manufacturer's instructions. DNA isolated from ear cuts was mixed 1:50 with 0.5 µM of forward (5'-ACCCAGGACAGTGAGAC-3') and reverse (5'-GCTTTGCAGCAGCTCGTTC-3') primers (Bio-Rad) and iQ SYBR green supermix (Bio-Rad). The qPCR reaction was performed at 95°C for 5 min, 35 cycles of 95°C for 30 sec, 55°C for 15 sec and 69°C for 30 sec, followed by a melt curve from 81°C to 86°C with increments of 0.2°C every 5 sec using a CFX384 Touch real-time PCR detection system (Bio-Rad). Since after *Cre-loxP*-mediated recombination one *loxP* site (consisting of 117 base pairs, including the 34 base pairs of the *loxP* site) remains present in the R14del *Pln* allele, presence of the WT and/or mutant allele is identified based on the size of the qPCR product (107 base pairs for the WT allele, 224 base pairs for the mutant allele), which can be distinguished based on the temperature of the melt peak (±83°C *vs*. ±85°C) using CFX Manager software (version 3.0; Bio-Rad). Validity of the melt peak identification has been confirmed by separation of qPCR products using agarose gel electrophoresis (2% agarose (Invitrogen, CA, USA) dissolved in Tris-acetate-ethylenediaminetetraacetic acid (EDTA) (TAE) buffer (40 mM Tris (Sigma-Aldrich, MO, USA), 20 mM glacial acetic acid (Merck Millipore, MA, USA) and 1 mM EDTA (Merck Millipore) in distilled water) with 0.5 µg/ml ethidium bromide (Sigma-Aldrich).

Echocardiography

Transthoracic echocardiography was performed using a Vevo imaging station (FUJIFILM VisualSonics, Canada) and a Vevo 3100 preclinical imaging system (FUJIFILM VisualSonics), equipped with a 40-MHz MX550D linear array transducer (FUJIFILM VisualSonics). Prior to echocardiographic imaging, mice were anesthetized (2% isoflurane (TEVA Pharmachemie) mixed with oxygen, administered via an aerial dispenser) and the hair was removed from the thorax using a commercially available topical depilation agent with potassium thioglycolate (Veet). Mice were fixed in supine position on the (37°C) temperature-maintained platform of the Vevo imaging station (FUJIFILM VisualSonics) over the integrated electrode pads to monitor the heart and respiration rates. LV parasternal long axis B-mode recordings and short axis M-mode recordings were obtained at the mid-papillary level. In addition, multiple serial short axis B-mode images were acquired along the long axis using default settings, covering the entire heart from apex to base with steps of 0.076 mm using the 3D motor stage (FUJIFILM VisualSonics) combined with automated respiration gating and electrocardiographic (ECG) triggering. Vevo LAB software (version 3.2.6; FUJIFILM VisualSonics) was used for image analysis. Serial short axis B-mode images were merged to generate three-dimensional (3D) LV volumetric reconstructions to analyze end-diastolic volume (EDV) and end-systolic volume (ESV) by delineating the end-diastolic and end-systolic endocardial borders using the multi-slice method combined with the closed spline method of the Vevo LAB software. Stroke volume (SV) was calculated as EDV - ESV, and ejection fraction (EF) was calculated as SV / EDV * 100%. Details of the validity and accuracy of 3D echocardiography have been reported elsewhere.[27] Parasternal long axis B-mode recordings were used for speckle-tracking analysis to evaluate global longitudinal strain (GLS) by outlining the epicardial and endocardial borders. Short axis M-mode recordings were used to determine heart rate, LV end-diastolic internal diameter (LVIDd), LV end-systolic internal diameter (LVIDs) and fractional shortening (FS) by outlining the epicardial and endocardial borders using the LV Trace tool. For two-dimensional (2D) measurements, three subsequent cardiac cycles, unaffected by respiration, were analyzed.

Surface electrocardiography

ECG recordings were acquired in LabChart Pro software (version 8; ADInstruments, New-Zealand) using two-lead subdermal needle electrodes connected to a PowerLab 8/30 data acquisition device (model ML870; ADInstruments) and an animal Bio Amp biological potential amplifier (model ML136; ADInstruments) with sampling rate 1 k/s, 1 kHz low-pass filter, 0.3 Hz high-pass filter and 2 mV range. Mice were anesthetized (2% isoflurane (TEVA Pharmachemie) mixed with oxygen, administered via an aerial dispenser) and fixed on a heating pad (37°C) in supine position. Recording needle electrodes were placed subdermally into the right axillary region (negative electrode) and the left inguinal region (positive electrode; lead II configuration). After a stabilization period of two minutes, a recording of one minute was acquired, which was considered sufficient to provide a representative view of heart function (400-600 cardiac cycles). RR, PR and QT intervals, P and QRS durations, P, Q, R, S and T amplitudes, ST height and heart rate were analyzed using the ECG Analysis module of the LabChart Pro software (version 8; ADInstruments). One-minute recordings were averaged by overlaying all cycles using QRS maximum for alignment. Noise-contaminated (due to movement artifacts) and abnormal waveforms were excluded from the analysis using the ECG Beat Classifier. ECG parameters were detected and measured automatically using the default detection and analysis settings for mice with adjusted maximum PR and RT times when necessary, and manually adjusted where appropriate in the ECG Beat Averaging View. QRS duration was measured from the start of the Q-wave to the end of the S-wave on the isoelectric line. As in rodents the T-wave directly succeeds the QRS complex, the end of the QRS complex marked the start of the T-wave. The QT interval was measured from the start of the Q-wave to the end of the T-wave, which was determined as the return of the signal to the isoelectric line. In contrast to humans, which show a pause between the QRS complex and T-wave, the ST segment is not clearly defined in mice. Therefore, ST height was measured according to the method provided by the LabChart software, in which the ST height was determined 10 ms after the R-wave peak, which served as alignment point for cardiac cycle averaging.

Sacrifice

Euthanasia was performed by exsanguination. Briefly, after mice were anesthetized, the abdomen was opened, the aorta was cut, and the circulation was perfused with saline. The heart was quickly excised, rinsed in a KCl solution (1 M KCl (Merck Millipore) in demiwater) to arrest the heart in diastole, weighed and dissected. A transverse mid-slice was fixed overnight in 4% buffered formaldehyde solution (10% formalin; Klinipath, the Netherlands) for histological analysis. Remaining LV tissue was snap-frozen in liquid nitrogen, and stored at -80°C until further processing. Tibias were collected from the right hind leg, and tibia lengths were determined using a caliper. Organ weights were indexed by tibia length to the power 3 to normalize for body size.[14]

Histological analysis

After sacrifice, a transverse mid-slice of the heart (±1 mm thick) was fixed overnight in 10% formalin (Klinipath). Next, formalin-fixed tissues were processed using a Leica TP1020 automated tissue processor (Leica Microsystems, Germany). Samples were subjected to a dehydration series (70% ethanol (Klinipath) for 1 h, 80% ethanol for 1 h, 90% ethanol for 1 h, and three times 100% ethanol for 1 h) to remove most of the water from the samples, and cleared from ethanol by washing three times with xylene (Klinipath) for 1 h, followed by two 1-h infiltrations with histological paraffin wax (Klinipath). Processed tissue samples were subsequently embedded in histological paraffin wax (Klinipath) using a Leica EG1150 H paraffin embedding module (Leica Microsystems). Embedded tissue slices were cut into 4-µm thick transversal sections using a Leica RM2255 microtome (Leica Microsystems), and mounted on StarFrost Adhesive silane-coated microscope slides (Waldemar Knittel Glasbearbeitungs, Germany). Sections were incubated overnight at 60°C for deparaffinization of the tissues. For complete deparaffinization and rehydration of the tissues, sections were incubated in xylene for 20 min, 100% ethanol for 10 min, 96% ethanol for 5 min, 70% ethanol for 1 min, and rinsed with distilled water before histological analysis.

Masson's trichrome stain was performed to detect collagen deposition as a measurement of fibrosis. Nuclei were stained black by incubation in Weigert's iron hematoxylin solution (0.5% hematoxylin solution (Gill no. I; Sigma- Aldrich), 0.06% $FeCl_3$ (Sigma-Aldrich) and 0.5% HCl (Merck Millipore) in distilled water) for 10 min. Sections were washed in running tap water for 10 min and rinsed with distilled water. Next, cytoplasm was stained red by incubation in Biebrich scarlet-acid fuchsin solution (0.9% Biebrich scarlet (VWR Chemicals, PA, USA), 0.1% acid fuchsin (Sigma-Aldrich) and 0.5% glacial acetic acid (Merck Millipore) in distilled water) for 13 min. Sections were washed twice with distilled water before differentiation in phosphomolybdic-phosphotungstic (PP) acid solution (3% phosphomolybdic acid hydrate (Alfa Aesar, MA, USA) and 2.5% phosphotungstic acid (Sigma-Aldrich) in distilled water) for 14 min. Without rinsing, sections were transferred to aniline blue solution (1.26% aniline blue (Acros Organics, Belgium) and 2% glacial acetic acid in distilled water) for 7 min to stain collagen blue. Sections were washed twice with distilled water before differentiation in 1% glacial acetic acid solution for 4 min. Subsequently, sections were rinsed with distilled water, and dehydrated in 96% ethanol for 15 sec, 100% ethanol for 2 min and xylene for 10 min. Sections were covered with DPX (a mixture of distyrene, a plasticizer (tricresyl phosphate) and xylene) neutral mounting medium (Sigma-Aldrich) and a cover slip. To quantify the amount of fibrosis, whole stained sections were automatically imaged using a NanoZoomer 2.0-HT digital slide scanner (Hamamatsu Photonics, Japan), and fibrotic area was determined using the Positive Pixel Count v9 algorithm of Aperio's ImageScope software (version 12.4.0; Leica Microsystems) with default settings, hue value 0.66 and hue width 0.2. Fibrosis fractions were quantified as a percentage of the total area of the entire stained section, and calculated as fold change compared to the age-matched control group.

To visualize PLN protein aggregates, immunofluorescent staining for PLN was performed using a mouse monoclonal anti-PLN antibody (clone 2D12; #MA3-922, Invitrogen), which has been shown to recognize (aggregated) PLN-R14del proteins,[7,8,16] labeled with Alexa Fluor 555 (red) using an APEX antibody labeling kit (Invitrogen) according

to the manufacturer's protocol. The anti-PLN antibody was loaded onto the prehydrated resin of the APEX antibody labeling tip together with the fluorescent label, and incubated for 2 h at room temperature, followed by elution of the labeled antibody. Tissue sections were washed three times in phosphate-buffered saline (PBS; 1.76 mM KH_2PO_4 (Merck Millipore), 10 mM Na_2HPO_4 (Sigma-Aldrich), 136.9 mM NaCl (Merck Millipore) and 2.68 mM KCl (Merck Millipore) in distilled water) for 5 min. Antigen retrieval was performed by incubating sections for 15 min in boiling antigen retrieval buffer (10 mM Tris (Sigma-Aldrich) and 1 mM EDTA (Merck Millipore) in distilled water; TE buffer). After cooling down, excess antigen retrieval buffer was removed by washing three times in PBS for 5 min. Next, sections were incubated with fluorescently labeled anti-PLN antibody (1:200) to stain PLN red, and fluorescein isothiocyanate (FITC)-conjugated wheat germ agglutinin (WGA) (2 mg/ml in PBS, 1:100; Sigma-Aldrich) for 1 h in the dark to stain extracellular matrix (ECM) green. After rinsing excess antibody three times with PBS for 10 min, sections were incubated in VECTASHIELD mounting medium with 4',6-diamidino-2-phenylindole (DAPI; Vector Laboratories, CA, USA) for 30 min to stain nuclei blue. Sections were covered by a cover slip, which was sealed using blank nail polish, and stored at 4°C protected from light until imaging. Fluorescent imaging was done using a Leica AF6000 fluorescence imaging system (Leica Microsystems).

Quantitative polymerase chain reaction

RNA was isolated from snap-frozen LV tissues using TRI Reagent (Sigma-Aldrich) according to the manufacturer's protocol. Snap-frozen LV tissues were mechanically disrupted, and approximately 25 mg of powdered LV tissue was homogenized in 1 ml of TRI Reagent (Sigma-Aldrich) using a TissueLyser LT (Qiagen, Germany) at 50 Hz for 5 min. After incubation for 5 min at room temperature to ensure complete dissociation of nucleoprotein complexes, phases were separated by thoroughly mixing with 0.2 ml chloroform (Merck Millipore), incubation for 2 min at room temperature, and centrifugation at 12,000 *g* for 15 min at 4°C. The RNA-containing colorless upper aqueous phase was isolated and RNA was precipitated by mixing with 0.5 ml 2-propanol (Biosolve, the Netherlands) and incubation for

10 min at room temperature, followed by centrifugation at 12,000 *g* for 10 min at 4°C. The supernatant was discarded, and the RNA pellet was washed twice by mixing with 1 ml 75% ethanol (Merck Millipore) and centrifugation at 12,000 *g* for 5 min at 4°C. The supernatant was removed, and the RNA pellet was air-dried before dissolving in RNase-free water. RNA concentrations were determined by spectrophotometry using a NanoDrop 2000 spectrophotometer (Thermo Scientific, MA, USA).

Next, cDNA synthesis was performed using QuantiTect reverse transcription (RT) kit (Qiagen) following manufacturer's instructions. For every sample, 200 ng of isolated total RNA was incubated with gDNA wipe-out buffer (Qiagen) at 42°C for 2 min to remove any contaminating genomic DNA. After gDNA elimination, the purified RNA samples were converted to cDNA by reverse transcription by adding Quantiscript reverse transcriptase (Qiagen) and RT primer mix (Qiagen) in Quantiscript RT buffer (Qiagen). The RT reaction was performed at 42°C for 15 min and was subsequently inactivated at 95°C for 3 min using a T100 thermal cycler (Bio-Rad).

Gene expression levels were determined by qPCR analysis using iQ SYBR green supermix (Bio-Rad) according to the manufacturer's instructions. Duplicates of 7.5 ng cDNA were mixed with 750 nM forward and reverse primers and iQ SYBR green supermix (Bio-Rad). Primers that were used, included 5'-GCTTCCAGGCCATATTGGAG-3' (forward) and 5'- GGTGGTCTAGCAGGTTCTTG-3' (reverse) for *Nppa* (atrial natriuretic peptide, ANP) and 5'-AAGCGCGTCCTGGCATTGTC-3' (forward) and 5'- GCAGCCGCAAATGCAGATGG-3' (reverse) for *Rplp0* (36B4) (Bio-Rad). The qPCR reaction was performed at 95°C for 3 min followed by 35 cycles of 95°C for 15 sec and 60°C for 30 sec using a CFX384 Touch real-time PCR detection system (Bio-Rad). Gene expression was quantified by correcting for reference gene values of one of the components of the large 60S ribosomal subunit (*Rplp0*) using CFX Manager software (version 3.0; Bio-Rad), and the calculated values were expressed relative to the age-matched control group.

Western blot

For protein isolation, snap-frozen LV tissues were mechanically disrupted, and approximately 25 mg of powdered tissue was homogenized in 0.2 ml ice-cold radioimmunoprecipitation assay (RIPA) lysis buffer (50 mM Tris (Sigma-Aldrich), 1.0% IGEPAL CA-630 (Sigma-Aldrich), 0.5% sodium deoxycholate (Sigma-Aldrich), 0.1% sodium dodecyl sulfate (SDS) (Sigma-Aldrich) and 150 mM NaCl (Merck Millipore) in distilled water) freshly supplemented with 4% cOmplete protease inhibitor (PI) cocktail (Roche Diagnostics, Switzerland), 1% phosphatase inhibitor cocktail 3 (Sigma-Aldrich), 15 mM sodium orthovanadate (Sigma-Aldrich), and 1 mM phenylmethylsulphonyl fluoride (PMSF) (Roche Diagnostics) using a TissueLyser LT (Qiagen) at 50 Hz for 5 min. After centrifugation at 12,000 *g* for 10 min at 4°C, the supernatant containing SDS-solubilized proteins was collected. The remaining pellet, which contains SDS-insoluble proteins, was dissolved in 50 µl urea solution (8 M urea (Sigma-Aldrich), 0.1 M NaH_2PO_4 (Merck Millipore) and 0.01 M Tris-HCl (Sigma-Aldrich) in distilled water) complemented with 1.25 U Pierce Universal nuclease for cell lysis (Thermo Scientific). Since protein aggregates are present in the cardiomyocytes of PLN-R14$^{\Delta/\Delta}$ mice, and it is yet unknown what the exact contents of these aggregates are, we combined the RIPA-soluble and RIPA-insoluble fractions into total protein lysates to prevent protein expression levels from being affected by protein (in)solubility.

Protein concentrations were determined using a Pierce bicinchoninic acid (BCA) protein assay kit (Thermo Scientific) according to the manufacturer's protocol. Duplicates of protein samples were mixed 1:200 (v:v) with working reagent (50 reagent A : 1 reagent B) in a flat-bottom 96-wells plate and incubated at 37°C for 30 min for the proteins to reduce Cu^{2+} to Cu^{1+} (biuret reaction), which is chelated with two BCA molecules. Absorbance of the purple-colored reaction product was measured at 562 nm using a Synergy H1 microplate reader (BioTek, VT, USA). Absorbance values were corrected for the average absorbance value of a blank sample (lysis buffer), after which protein sample concentrations were determined based on a standard curve of bovine serum albumin (BSA) samples with known concentrations using a linear curve fit using Gen5 software (BioTek).

Protein expression levels were determined by Western blotting. Equal amounts of proteins (15 µg) with sample buffer (2% SDS (Sigma-Aldrich), 8% glycerol (Sigma-Aldrich), 60 mM Tris (Sigma-Aldrich), 20 mM dithiothreitol (DTT) (Sigma-Aldrich) and 0.5 mg bromophenol blue (Sigma-Aldrich) in demiwater) were denatured at 95°C for 5 min and separated by SDS-polyacrylamide gel electrophoresis (PAGE) on ice using handcast gels (stacking gel: 0.1% SDS (Sigma-Aldrich), 125 mM Tris (Sigma-Aldrich), 4% acrylamide (Sigma-Aldrich), 0.3% ammonium persulfate (APS) (Sigma-Aldrich) and 0.04% tetramethylethylenediamine (TEMED) (Carl Roth, Germany) in demiwater; separation gel: 0.1% SDS (Sigma-Aldrich), 375 mM Tris (Sigma-Aldrich), 15% acrylamide (Sigma-Aldrich), 0.1% APS (Sigma-Aldrich) and 0.1% TEMED (Carl Roth) in demiwater) and electrophoresis buffer (0.1% SDS (Sigma-Aldrich), 25 mM Tris (Sigma-Aldrich), 192 mM glycine (Sigma-Aldrich) in demiwater) in a mini-PROTEAN system (Bio-Rad). Separated proteins were transferred onto Immun-Blot polyvinylidene fluoride (PVDF) membranes (pore size 0.2 µm; Bio-Rad) by semi-dry blotting using transfer buffer (25 mM Tris (Sigma-Aldrich), 192 mM glycine (Sigma-Aldrich) and 20% methanol (VWR Chemicals) in demiwater). After transfer, total protein levels for each sample were determined using Revert 700 Total Protein Stain (LI-COR Biosciences, NE, USA), according to the manufacturer's instructions. Next, membranes were blocked in block buffer (5% dry-milk (Campina, the Netherlands) in Tris-buffered saline (TBS) (150 mM NaCl (Merck Millipore) and 10 mM Tris (Sigma-Aldrich) in distilled water) with 0.1% TWEEN (polysorbate) 20 (Sigma-Aldrich) (TBST)) for a minimum of 1 h at room temperature while shaking and incubated overnight at 4°C while shaking with an anti-proANP primary antibody (ab91250, Abcam, UK) diluted 1:200 in block buffer. To remove unbound primary antibody, membranes were washed three times in TBST for 5 min while shaking, followed by 1-h incubation at room temperature while shaking with an anti-rabbit horseradish peroxide (HRP)-linked secondary antibody (P044801, Dako, CA, USA) diluted 1:2,000 in block buffer. After washing off unbound secondary antibody, detection was performed using Immobilon Classico Western HRP substrate (Merck Millipore) and an ImageQuant LAS 4000 digital imaging system (GE Healthcare, IL, USA).

RNA sequencing

Total RNA was isolated from snap-frozen LV tissues using TRI Reagent (Invitrogen) according to the manufacturer's protocol as previously mentioned for qPCR. Total RNA quality was assessed using an RNA 6000 Pico Kit (Agilent Technologies, CA, USA) with a 2100 Bioanalyzer instrument (Agilent Technologies) following the manufacturer's instructions. Nucleic acid fragments in 1 µl of RNA samples were separated together with the provided ladder (Agilent Technologies) based on their size by electrophoresis through the RNA microfluidic chip (Agilent Technologies). The RNA Integrity Number (RIN) of the RNA samples was automatically determined based on the electropherogram of the gel using the 2100 Expert software (Agilent Technologies). All RNA samples had a RIN value ≥7.2. mRNA libraries were generated using a TruSeq Stranded mRNA Library Prep kit (Illumina, CA, USA) according to the manufacturer's protocol. Poly-A-containing mRNA molecules were purified from 1 µg of total RNA using poly-T oligo-attached magnetic beads, fragmented, converted to cDNA, adenylated on the 3' end, ligated with adaptors, and amplified using PCR. Libraries were quantified, normalized, pooled and subjected to single-end sequencing (1 x 75 bp) using a NextSeq 500 Sequencing System (Illumina). Raw sequence FastQ files underwent read quality assessment with FastQC (version 0.11.8) (https://www.bioinformatics.babraham.ac.uk/projects/fastqc/). Trimming of Illumina adapters and low-quality was performed on the resulting sequencing reads using TrimGalore (version 0.6.5) (http://www.bioinformatics.babraham.ac.uk/projects/trim_galore/). SortMeRNA (version 4.2.0) was used to remove sequencing reads from ribosomal origins.[41] Reads were aligned to the genome reference consortium mouse build 38 (GRCm38; mm10) using spliced transcript alignment to a reference (STAR, version 2.7.3a).[42] Alignments were assessed for quality with RSeQC (version 3.0.1),[43] and for library complexity saturation with Preseq (version 2.0.3).[44] The featureCounts function of the SubRead (version 2.0.0) package was used for read summarization to assign mapped reads to exons.[45] Count data was normalized, and differential gene expression analysis of normalized count data, clustering analysis and principle component analysis (PCA) were performed using the DESeq2

package (version 1.28.1) in R (version 4.0.2).[21] Size factor and dispersion estimation were performed with default settings. *P*-values were calculated using Wald test and corrected for multiple testing using the Benjamini-Hochberg method. Gene set enrichment analysis (GSEA) was performed using the fgsea package (version 1.14.0) with default settings (gene set size 15 to 500) in R using the biological processes subset of the Gene Ontology (GO) gene sets of the Molecular Signatures database (MSigDB; version 7.0).[22]

Mass spectrometry

For proteomics analysis, proteins were analyzed by liquid chromatography tandem-mass spectrometry (LC-MS/MS). Cardiac tissues were diced on dry ice, and washed four times with PBS (Lonza, Switzerland) supplemented with 1:100 (v:v) broad-spectrum protease inhibitor cocktail (Sigma-Aldrich) and phosphatase inhibitors (Roche Diagnostics) to minimize blood contamination. Tissues were homogenized in 0.3-0.5 ml lysis buffer (19 mM Tris (Sigma-Aldrich), 113 mM NaCl (Sigma-Aldrich), 2 mM egtazic acid (EGTA; Sigma-Aldrich), 5 mM EDTA (Sigma-Aldrich), 1% Triton (Sigma-Aldrich) and 0.1% SDS (Sigma-Aldrich), complemented with 1:100 (v:v) protease inhibitor cocktail and phosphatase inhibitors) using Lysing Matrix D ceramic beads (MP Biomedicals, CA, USA) and a Precellys tissue homogenizer (Bertin Technologies, France). Protein lysates were centrifuged twice at 16,000 *g* for 10 min at 4°C, and the supernatant was isolated. Protein concentrations were determined using a Pierce BCA protein assay kit according to the manufacturer's protocol as described for Western blot. Next, 20 µg of proteins were denatured using 6 M urea (Calbiochem, CA, USA) and 2 M thiourea (Merck Millipore), and reduced using 10 mM DTT (Sigma-Aldrich) by incubation for 1 h at 37°C with agitation at 240 rpm, followed by alkylation for 1 h at room temperature while protected from light using 50 mM iodoacetamide (Sigma-Aldrich). Proteins were precipitated overnight at -20°C using pre-chilled acetone (1:9 v:v; Sigma-Aldrich), and subsequently centrifuged at 16,000 *g* for 30 min at 4°C. The supernatant was discarded, and protein pellets were dried using a Savant SPD131DDA SpeedVac Concentrator (Thermo Scientific) and dissolved in 0.1 M triethyl ammonium bicarbonate

(TEAB) buffer (Sigma-Aldrich). Proteins were digested overnight at 37°C with agitation at 240 rpm using 0.8 µg Trypsin/Lys-C mix (1:25 enzyme:protein; Promega, WI, USA). Protein digestion was terminated using a final concentration of 1% trifluoroacetic acid (TFA; Thermo Scientific) to lower the pH. C18 peptide clean-up was performed using AssayMAP C18 cartridges (Agilent Technologies) with an AssayMAP Bravo Protein Sample Prep platform (Agilent Technologies) according to the manufacturer's protocol. After the C18 cartridges were primed with 50% acetonitrile (ACN; Fisher Optima) and 0.1% TFA in LC-MS grade H_2O, and equilibrated with 1% ACN and 0.1% TFA in LC-MS grade H_2O, protein digests were loaded and washed with 1% ACN and 0.1% TFA in LC-MS grade H_2O, then eluted in 70% ACN and 0.1% TFA in LC-MS grade H_2O. Eluted peptides were dried using a vacuum concentrator, and dissolved in 0.1 M TEAB buffer. Cleaned peptides were labeled with Tandem Mass Tag (TMT) 10plex isobaric compounds (Thermo Scientific) for protein identification and quantitation following manufacturer's instructions. Briefly, TMT Label Reagent was added to the peptides and incubated for 1 h at room temperature before quenching the reaction using a final concentration of 0.25% hydroxylamine (Sigma-Aldrich) for 15 min at room temperature. Samples labeled with 10 different TMT tags were pooled together and dried using a vacuum concentrator, and dissolved in 0.1% triethylamine (TEA; Fisher Scientific). Samples were fractionated using high pH reversed phase high performance liquid chromatography (RP-HPLC) using a ZORBAX Extend 300-C18 RP HPLC column (4.6 mm inner diameter x 150 mm length, 3.5 µm particle size; Agilent Technologies), and 8 fractions were collected for each TMT 10plex mixture. Peptide fractions were dried and reconstituted in 2% ACN and 0.05% TFA in LC-MS grade H_2O. Next, on average 2.5 µg of each fraction were injected and separated by an UltiMate 3000 Rapid Separation Liquid Chromatography (RSLC)nano system (Thermo Scientific) on an EASY-Spray RP C18 HPLC column (75 µm inner diameter x 50 cm length, 2 µm particle size; Thermo Scientific) using a 2 h LC gradient: 0-10 min 4-10% B, 10-75 min 10-30% B, 75-80 min 30-40% B, 80-85 min 40-99% B, 85-90 min 99% B, 90-120 min 4% B, where A = 0.1% formic acid (FA; VWR Chemicals) in H_2O, and B = 0.1% FA and 80% ACN in H_2O, with a flow rate of 250 nl/min

and a column temperature of 45°C. Separated peptides were directly sprayed into an Orbitrap Fusion Lumos Tribrid Mass Spectrometer (Thermo Scientific), and analyzed using the synchronous precursor selection (SPS)-based MS/MS/MS (MS3) workflow for TMT-labeled samples. Full MS spectra were collected on the Orbitrap (Thermo Scientific) with resolution 120,000 and scan range 375-1500m/z. The most abundant precursor ions were fragmented using collision induced dissociation (CID), and MS2 spectra were collected on a linear ion trap with dynamic exclusion enabled. The 5 most abundant fragment ions from every MS2 spectrum were selected and fragmented at the same time using the higher energy collisional dissociation (HCD) fragmentation method with 65% collision energy, and MS3 spectra were collected on the Orbitrap (Thermo Scientific) with resolution 60,000 and scan range 110-500m/z to measure the TMT reporter ions with 2 sec cycle time. Raw data were analyzed using Proteome Discoverer v2.3 (Thermo Scientific). All fractions of each TMT mixture were loaded and analyzed together. Each TMT tag was assigned to the correct sample and group. Data were searched against mouse UniProtKB/Swiss-Prot database (version 2019_01; 17,006 protein entries) using the Mascot search engine (version 2.6.0; Matrix Science) with enzyme trypsin, max. 2 missed cleavages, 10 ppm precursor mass tolerance, 0.8 Da fragment mass tolerance, carbamidomethylation on cysteine and TMT 6plex on N-terminal and lysine as static modifications, oxidation on methionine as dynamic modifications, and reporter ions S/N were used for quantification. Quantification values were normalized to total peptide amount, and scaled on the pooled control samples. The dataset was filtered to keep only proteins with less than 30% missing values or with more than 90% missing values in one phenotype and less than 10% in all other phenotypes. In the latter case, missing values of the phenotype which presented more than 90% of missing values were imputed with zeros. All remaining missing values were imputed using the k-Nearest Neighbor (K-NN) algorithm with k equal to 5 (default value) as implemented in the scikit-learn package (version 0.19.2) in Python.[46] The limma package (version 3.44.3) in R (4.0.2) has been used to compare between different phenotypes using the Empirical Bayes (eBayes) method.[24] Initial *p*-values were adjusted for multiple testing using the Benjamini-Hochberg

method. PCA for feature extraction using the scikit-learn Python library[46] scree test[47] was used to retain an adequate number of principal components to maintain at least the 90% variability of the data set. The Matplotlib Python package[48] was used to visualize all samples in the three-dimensional space formed by the three most significant principal components. Enrichment analysis was conducted using the Database for Annotation, Visualization and Integrated Discovery (DAVID) functional annotation tool.[25] This analysis included biological process terms from the GO knowledgebase,[49,50] and significantly enriched terms were inferred with Benjamini-Hochberg adjusted *q*-values of 10%.

Supplemental Figures

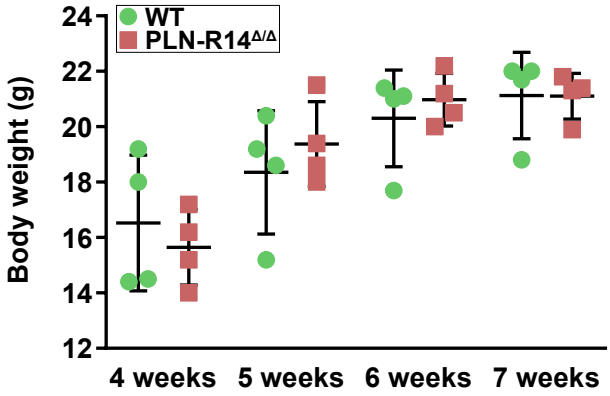

Supplemental Figure I. Body weights of male WT and PLN-R14$^{\Delta/\Delta}$ mice subjected to echocardiography and ECG at 4, 5, 6 and 7 weeks of age (n=4 per group). Data are presented as mean ± standard deviation (SD).

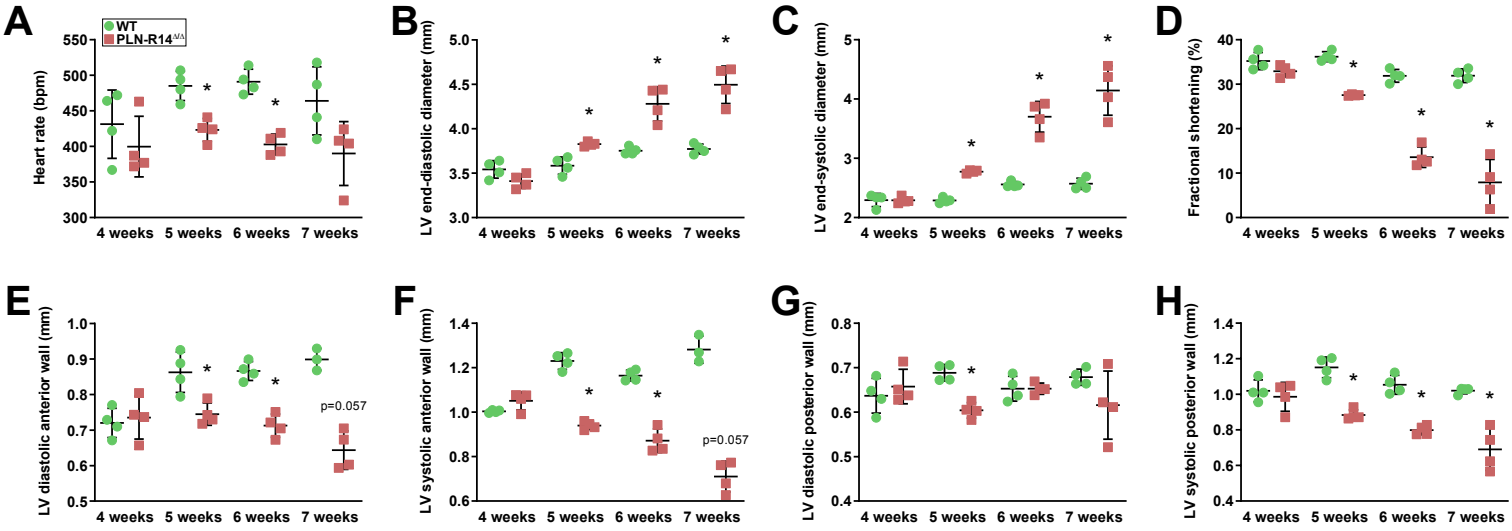

Supplemental Figure II. Two-dimensional short axis M-mode echocardiographic analysis, including heart rate **(A)**, LV end-diastolic and end-systolic internal diameters **(B,C)**, fractional shortening **(D)**, and end-diastolic and end-systolic anterior and posterior wall thicknesses **(E-H)** of 4- to 7-week-old male WT and PLN-R14$^{\Delta/\Delta}$ mice (n=4 per group, except n=3 for diastolic and systolic anterior wall thicknesses of 7-week-old WT mice). Data are presented as mean ± SD. *p<0.05 versus age-matched WT mice (Mann-Whitney test).

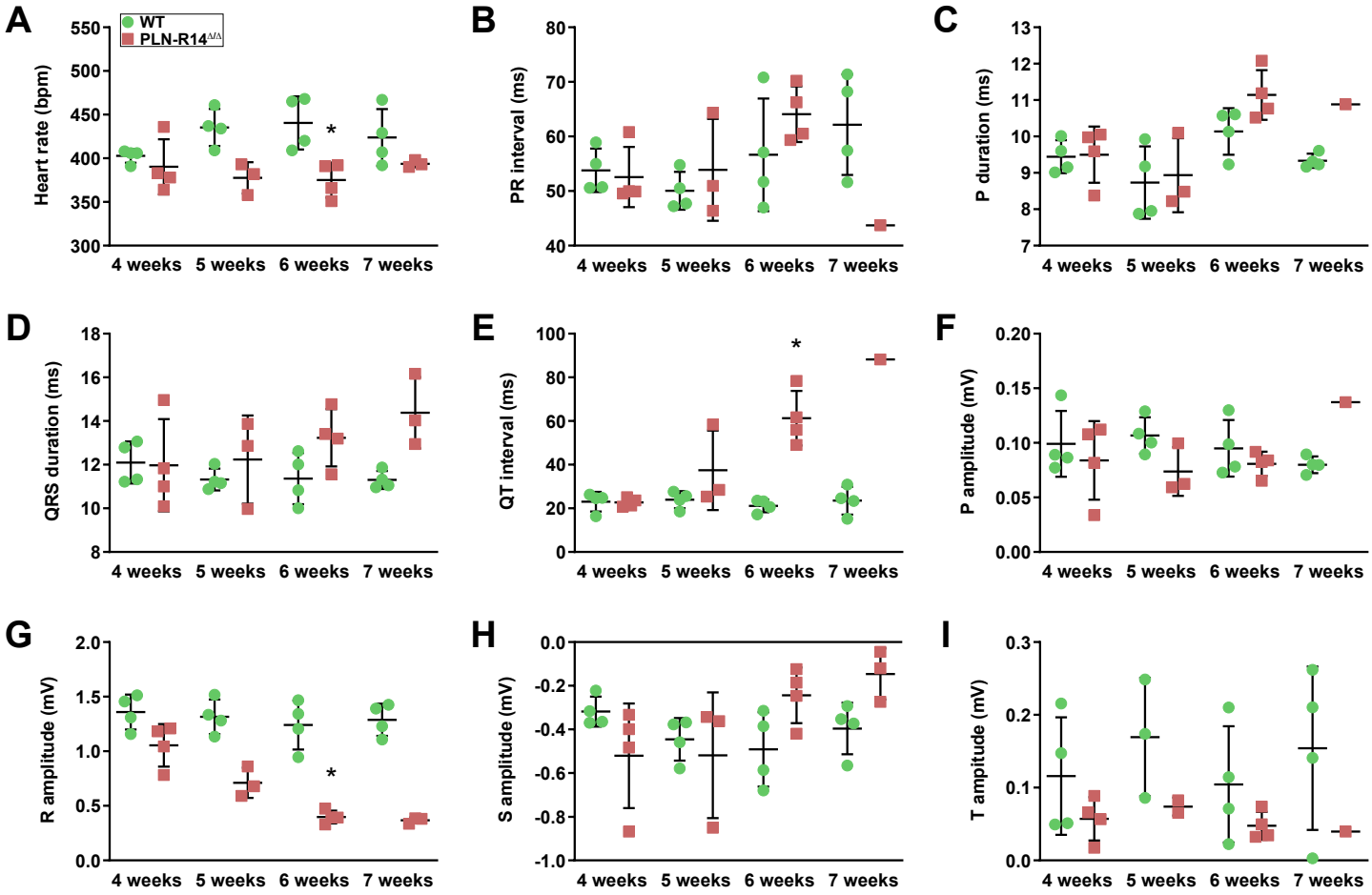

Supplemental Figure III. ECG parameters, including heart rate **(A)**, PR interval **(B)**, P duration **(C)**, QRS duration **(D)**, QT interval **(E)**, and P, R, S and T amplitudes **(F-I)** of 4- to 7-week-old male WT and PLN-R14$^{\Delta/\Delta}$ mice (n=4 per group, except n=3 for 5-week-old PLN-R14$^{\Delta/\Delta}$ mice, and n=1 for P- and T-wave parameters of 7-week-old PLN-R14$^{\Delta/\Delta}$ mice). Data are presented as mean ± SD. *p<0.05 versus age-matched WT mice (Mann-Whitney test).

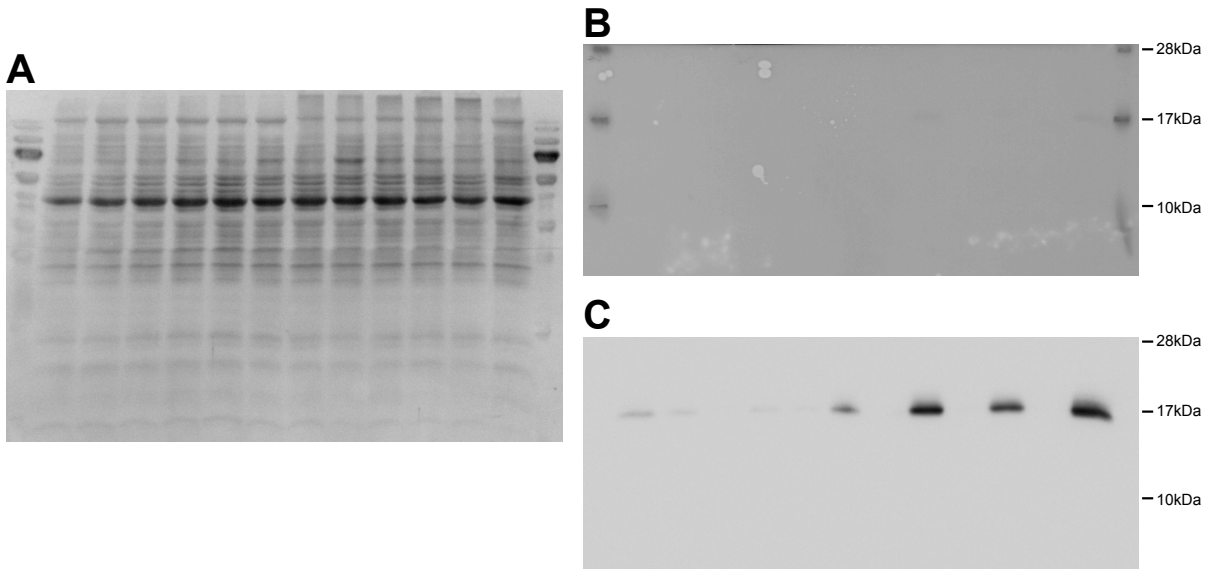

Supplemental Figure IV. Uncropped images of the Western blots shown in Figure 2G. **(A)** Visualization of total protein levels on the complete membrane. Subsequently, the membrane was cut in half at ~30kDa, and the bottom half was imaged digitally to show the prestained molecular weight markers **(B)**, followed by chemiluminescence detection of ANP protein levels **(C)**.

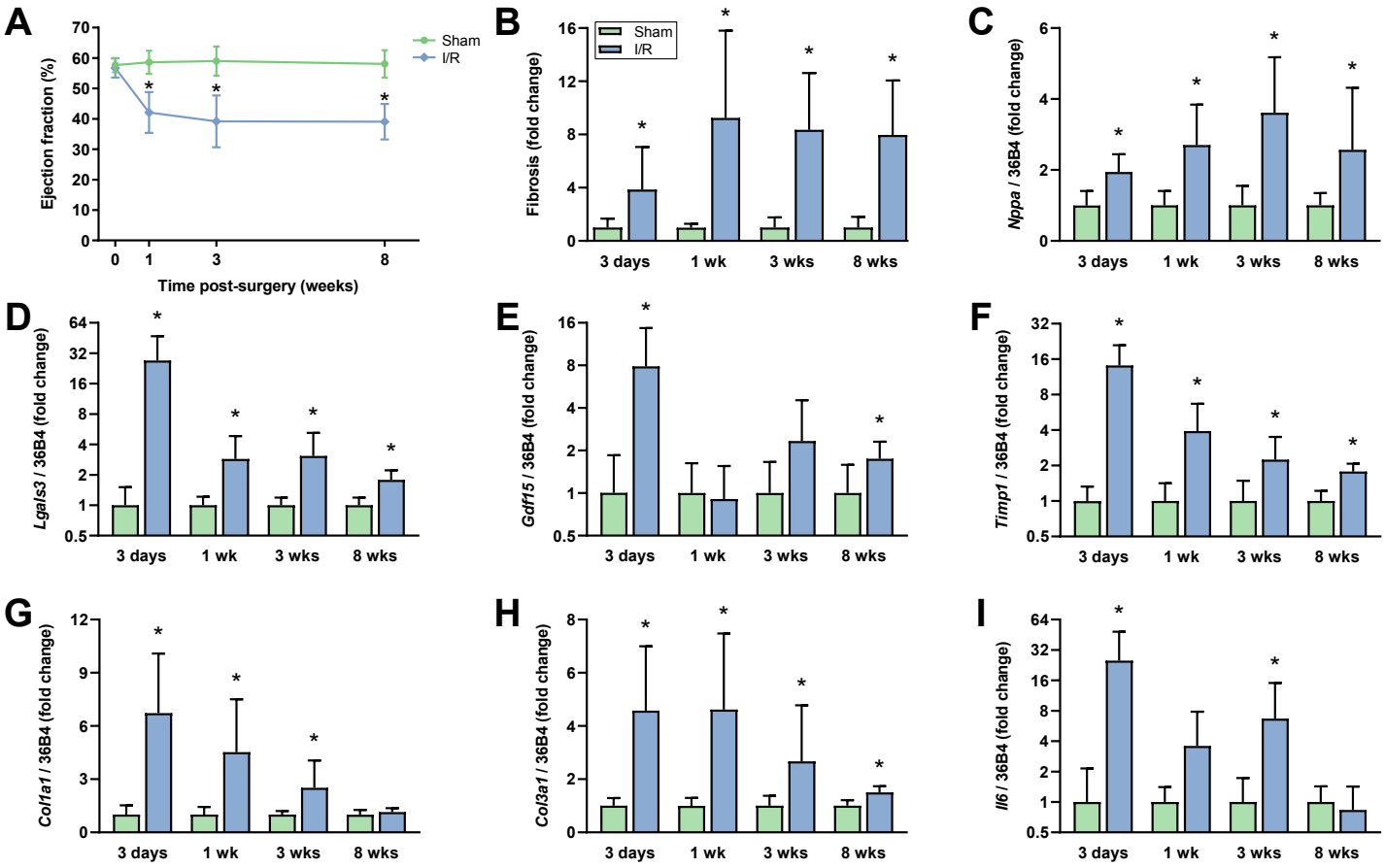

Supplemental Figure V. Cardiac function, remodeling and gene expression levels of male mice 3 days or 1, 3 or 8 weeks after sham or myocardial I/R surgery. **(A)** LVEF as determined by cardiac MRI (n=8-10). **(B)** Quantification of myocardial fibrosis as determined by Masson's trichrome-stained cardiac tissue sections. Data are presented as fold change compared to corresponding sham mice (n=8-10). **(C-I)** LV gene expression levels of *Nppa*, *Lgals3* (Gal-3, galectin-3), *Gdf15* (GDF15, growth differentiation factor 15), *Timp1* (TIMP1, tissue inhibitor of metalloproteinases 1), *Col1a1* (COL1A1, collagen type I alpha 1), *Col3a1* (COL3A1, collagen type III alpha 1) and *Il6* (IL-6, interleukin 6) as determined by qPCR (n=6-10). Gene expression values are corrected for *Rplp0* (36B4) gene expression, and shown as fold change compared to respective sham mice. Data are presented as mean ± SD. *p<0.05 versus corresponding sham mice. Gene expression levels of *Lgals3*, *Gdf15*, *Timp1* and *Il6* are shown on a logarithmic y-axis. Adapted from Du et al. *Theranostics* 2018;8(15):4155-4169.[10]

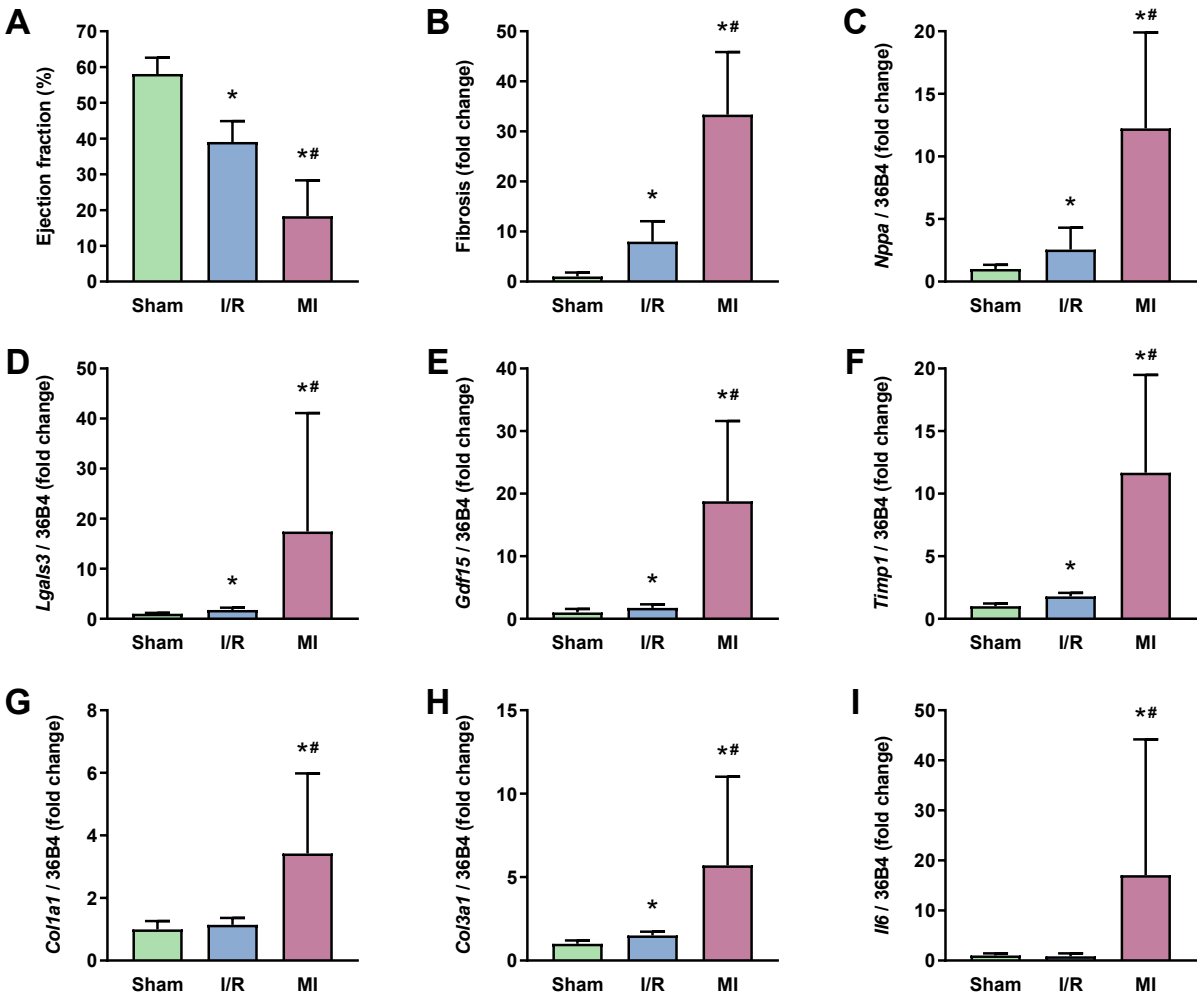

Supplemental Figure VI. Cardiac function, remodeling and gene expression levels of male mice 8 weeks after sham, myocardial I/R or MI surgery. **(A)** LVEF as determined by cardiac MRI (n=8-9). **(B)** Quantification of myocardial fibrosis as determined by Masson's trichrome-stained cardiac tissue sections. Data are presented as fold change compared to sham mice (n=8-9). **(C-I)** LV gene expression levels of *Nppa*, *Lgals3*, *Gdf15*, *Timp1*, *Col1a1*, *Col3a1* and *Il6* as determined by qPCR (n=6-9). Gene expression values are corrected for *Rplp0* gene expression, and shown as fold change compared to sham mice. Data are presented as mean ± SD. **p*<0.05 versus sham mice, $^{\#}p$<0.05 versus I/R mice. Adapted from Du et al. *Theranostics* 2018;8(15):4155-4169.[10]

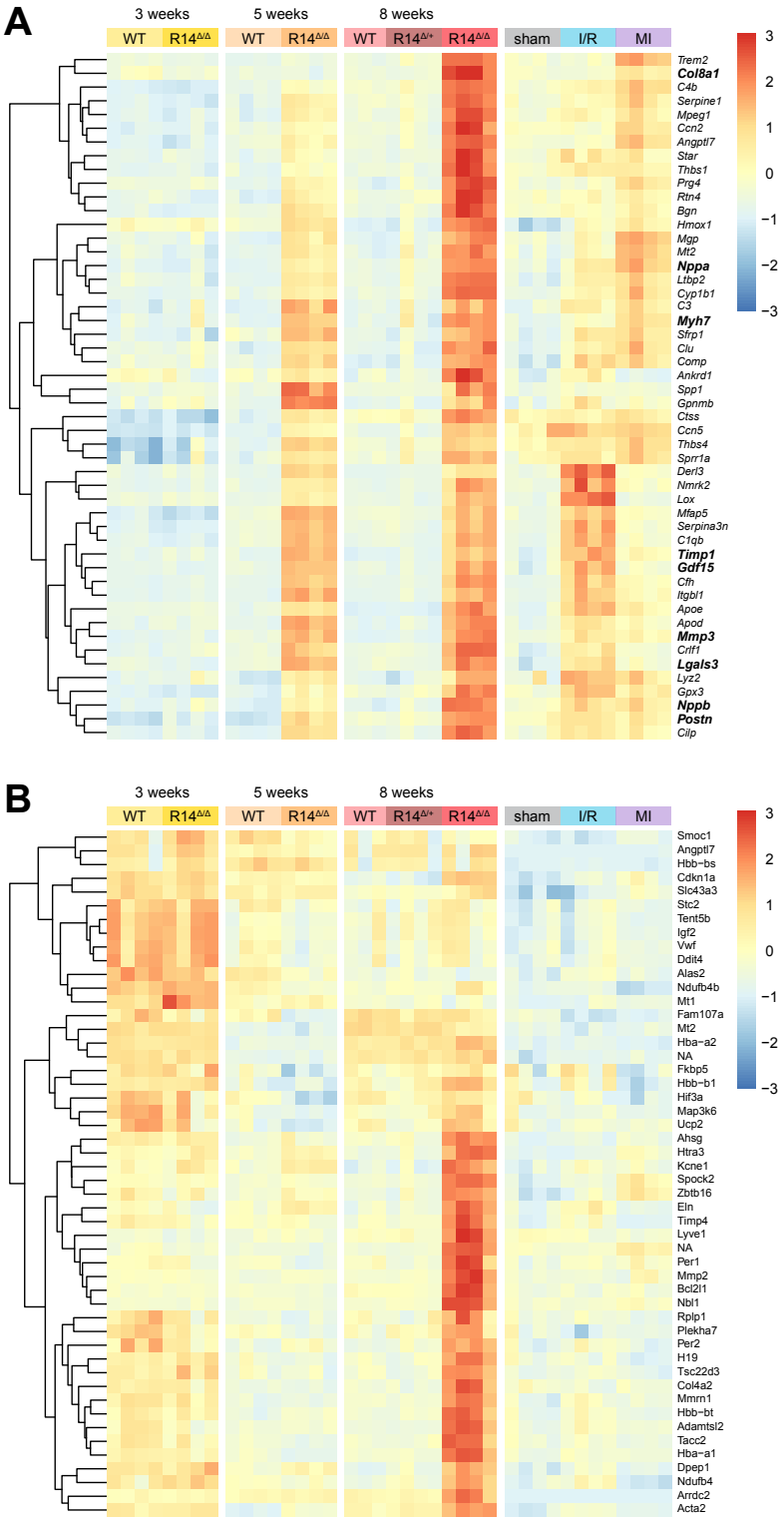

Supplemental Figure VII. Heatmaps of the top genes that contribute to the variance between 3-, 5- and 8-week-old WT and PLN-R14$^{\Delta/\Delta}$ hearts, 8-week-old PLN-R14$^{\Delta/+}$ hearts, and hearts 3 days after myocardial I/R injury, 8 weeks after MI surgery and 3 days or 8 weeks after sham surgery for the first principal component **(A)** or second principal component **(B)** of the PCA plot shown in Figure 3B.

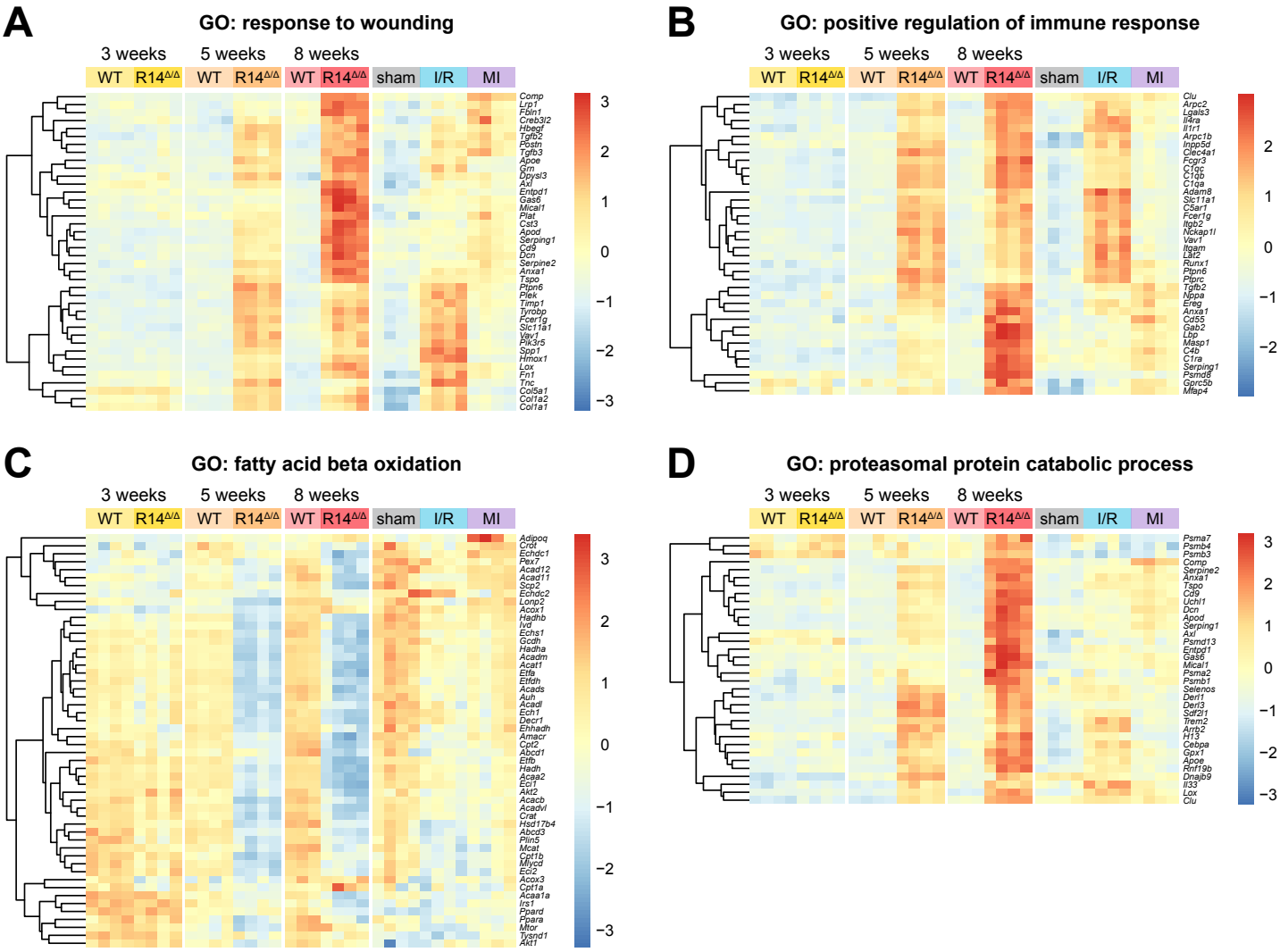

Supplemental Figure VIII. Heatmaps of the readcounts of leading-edge genes in 3-, 5- and 8-week-old WT and PLN-R14$^{\Delta/\Delta}$ hearts, and hearts 3 days after myocardial I/R injury, 8 weeks after MI surgery and 3 days or 8 weeks after sham surgery of enriched GO terms for biological processes that are significantly enriched in hearts of PLN-R14$^{\Delta/\Delta}$ mice and mice post-I/R or post-MI (shown in Figure 3E) **(A-C)**, or significantly differentially regulated exclusively in PLN-R14$^{\Delta/\Delta}$ hearts (shown in Figure 3F) **(D)**.

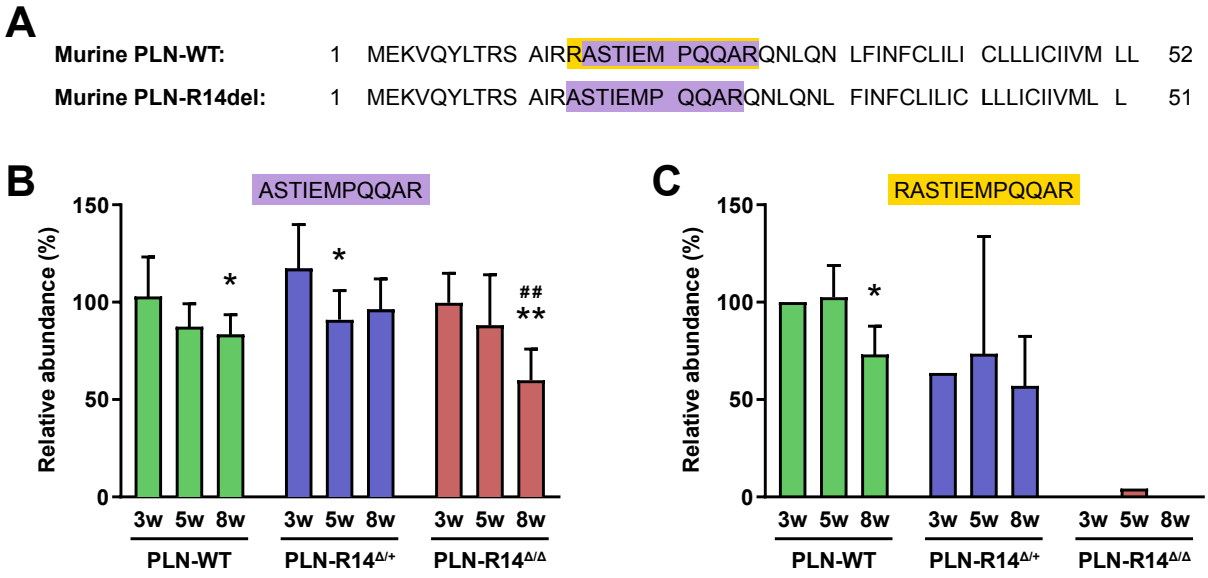

Supplemental Figure IX. (A) Murine PLN-WT and PLN-R14del protein amino acid sequences. Peptide products of trypsinization are marked in yellow (specific to PLN-WT) and purple (universal). **(B-C)** Relative abundance of ASTIEMPQQAR peptides (representing total PLN levels) **(B)** or RASTIEMPQQAR peptides (representing PLN-WT levels) **(C)** that were identified in LVs of 3-, 5- and 8-week-old male WT, PLN-R14$^{\Delta/+}$ and PLN-R14$^{\Delta/\Delta}$ mice by MS. Data are presented as mean ± SD. *p<0.05 and **p<0.01 versus 3-week-old mice of the same genotype; $^{\#\#}p$<0.01 versus WT mice of the same age (Kruskal-Wallis test).

Supplemental Tables

Supplemental Table I. RNA-Seq functional enrichment data of 3-week-old PLN-R14$^{\Delta/\Delta}$ mice hearts for terms that were identified exclusively in PLN-R14$^{\Delta/\Delta}$ mice.

Gene Ontology biological process term	Padj	NES	Leading-edge genes
GO_PROTEASOMAL_PROTEIN_CATABOLIC_PROCESS	0.0099	1.42	*SIAH2, **HSPA1B**, **HSPA1A**, PSMD12, FAM122A, PELI1, TRIM3, PSMC1, NFE2L2, CLU, CSNK1A1, ARNTL, WWTR1, PSMC2, PSMD1, RNF19B, FBXL16, **DDIT3**, PSMD3, NEDD4L, PSMD4, PRPF19, DDA1, SUMO1, PSMA6, **DERL3**, GID8, DVL1, UBQLN1, CTNNB1, PRKCG, UBE2J2, SIRT2, RHBDF1, TLK2, PSMA7, RYBP, RNF19A, TAF9, PSMD6, NSFL1C, PSMC5, HSP90AB1, UFD1, PSMD7, CSNK1E, GNA12, **PSMD5**, RCHY1, **PSMB1**, APOE, SOCS6, TAF1, OGT, USP7, SMAD7, CLOCK, RNF185, FBXO45, UBA52, CDC26, PSMA8, MAEA, SMARCC1, PSMA3, XPO1, SPSB3, DNAJB2, CDC23, FBXW7, ARIH1, PSMC4, ARIH2, IL33, UBXN4, TBL1X, CAMLG, FBXL5, SPSB4, NKD2, ATE1, PSMA5, PSMC6, PSMA1, PSMB4, RNF217, AMN1, **EDEM3**, CUL5, PMAIP1, UBXN8, KCTD10, **DERL1**, RMND5A, MTA1, FBXL4, PPP2CB, TOR1A, SIAH1, TMF1, NEMF, FBXL13, BAG2, FBXL12, **PSMD13**, SIRT1, ARMC8, PSMD11, ENC1, BAG5, ERLIN1, TMTC3, UBE2J1, UBE2W, YOD1, UBE2K, PLAA, PCBP2, UCHL1, MAP1A, PSMC3, RNF180, ERCC8, GPX1, RNF144A, PSME3, GET4, PLK2, PSMD8, SUMO2, SOCS4, AGAP3, FAF2, SYVN1, SMURF2, PLK3*
GO_REGULATION_OF_CELLULAR_AMINE_METABOLIC_PROCESS	0.0105	1.79	*PSMD12, PSMC1, AZIN1, PSMC2, NR4A2, PSMD1, PSMD3, PSMD4, PSMA6, PSMA7, PSMD6, ODC1, PSMC5, PSMD7, **PSMD5**, **PSMB1**, PSMA8, PSMA3, PSMC4, PSMA5, PSMC6, PSMA1, PSMB4, PDE1B, SLC7A11, **PSMD13**, PSMD11, PSMC3, PSME3, PSMD8, ATP2B4, **PSMA2**, PSMB2, PSMD2, PSMB6*
GO_PROTEIN_FOLDING	0.0102	1.55	***HSPA1B**, **HSPA1A**, HSP90AA1, CHORDC1, DNAJA1, HSPA8, PDCL3, DNAJC7, PSMC1, CLU, GNB3, ST13, DNAJB1, NPPB, PPIL2, PPIL6, HSPH1, PPIG, CWC27, PTGES3, DNAJC25, NKTR, DNAJC5, HSP90AB1, DNAJB6, FKBP9, MOGS, RANBP2, TRAP1, CCT3, DNAJB2, UNC45A, CSNK2A2, DNAJB5, CSNK2A1, HSPB1, PPID, NPPA, GRPEL2, P3H1, PDIA5, CCT8, TTC1, **DERL1**, DNAJC3, **DNAJB4**, GNAI3, TOR1A, PFDN5, BAG2, CCT4, RP2, BAG5, DNAJC24, CCT6A, HSPA2, CDC37, TBCC, SNRNP70, PDCD5, ERO1A, CHCHD4, SACS, DNAJC2, GNB2, HSPA1L, PPIA, NUDC, FKBP1B, SGTA, ATF6, PPIE, DNAJB12, P4HB*
GO_RESPONSE_TO_TOPOLOGICALLY_INCORRECT_PROTEIN	0.0091	1.55	*ATF3, **HSPA1B**, **HSPA1A**, HSP90AA1, DNAJA1, PTPN2, HSPA8, TATDN2, LMNA, NFE2L2, CLU, CREB3L1, DNAJB1, **DDIT3**, **DERL3**, TMEM33, HSPH1, **ATF4**, UBE2J2, EP300, HSP90AB1, UFD1, HYOU1, RNF185, XBP1, HDAC6, DNAJB2, COPS5, DNAJB5, HSF1, CCL2, UBXN4, THBS1, HSPB1, CREB3L2, NCK2, ZBTB17, HSPA4, OPTN, **EDEM3**, PPP1R15A, SERP1, PDIA5, NCK1, ADD1, **DERL1**, MANF, DNAJC3, **DNAJB4**, TOR1A, SSR1, UBE2W, YOD1, ATP6V0D1, CLPB, TSPYL2, PPP1R15B, HSPA2, FAF2, SYVN1, EXTL3, KLHL15, TBL2, HSPB8, ERO1A, ATXN3*
GO_INNATE_IMMUNE_RESPONSE_ACTIVATING_SIGNAL_TRANSDUCTION	0.0048	2.02	*RELB, PSMD12, MALT1, PSMC1, PSMC2, IKBKB, PSMD1, PSMD3, PSMD4, PSMA6, PLCG2, CREBBP, SRC, KRAS, EP300, PSMA7, PSMD6, PSMC5, PSMD7, PAK3, **PSMD5**, **PSMB1**, MUC3A, PSMA8, TAB2, PSMA3, PSMC4, RAF1, PDPK1, PSMA5, PSMC6, PSMA1, PSMB4, CHUK, **PSMD13**, PSMD11, CLEC4E, BCL10, PSMC3, HCK, PSME3, PSMD8, **PSMA2**, PSMB2, PSMD2, PSMB6*
GO_TUMOR_NECROSIS_FACTOR_MEDIATED_SIGNALING_PATHWAY	0.0048	1.88	***HSPA1B**, **HSPA1A**, KRT18, PTPN2, PSMD12, PSMC1, TRAF3, PSMC2, SPATA2, IKBKB, EDA2R, PSMD1, PSMD3, TNFRSF25, PSMD4, TNFRSF12A, PSMA6, TRAF2, LIMS1, PSMA7, PSMD6, PSMC5, NFKBIA, TRAF5, PSMD7, **PSMD5**, KRT8, TNFRSF19, **PSMB1**, PSMA8, OTULIN, PSMA3, KARS1, PLVAP, GPS2, PSMC4, COMMD7, PSMA5, PSMC6, PSMA1, EDA, PSMB4, TRAF4, TNFAIP3, TAX1BP1, CDIP1, CHUK, **PSMD13**, PSMD11, HIPK1, UBE2K, BIRC3, PSMC3, RIPK1, PSME3, PSMD8, PIAS4, **PSMA2**, PSMB2, GAS6, PSMD2, MAP3K14, PSMB6*
GO_LUNG_MORPHOGENESIS	0.0150	1.86	*SRF, STK40, CTNNB1, LIF, KRAS, SRSF6, SPRY1, NOG, ID1, YAP1, TCF21, SOX9, VANGL2, ESRP2, TNC, CELSR1, TGFBR2*
GO_INORGANIC_ION_IMPORT_ACROSS_PLASMA_MEMBRANE	0.0283	-1.67	*TRPM4, CACNA2D1, SLC5A1, ATP1A2, KCNJ12, KCNJ18, KCNJ3, CNGA3, WNK4, KCNH2, FXYD2, SLC9A5, TRPM2, KCNJ10, HCN4, SLC30A1, HFE, ATP1B3, SLC9A6, KCNJ11, TRPV2*
GO_FATTY_ACYL_COA_METABOLIC_PROCESS	0.0196	-1.85	*TECR, HSD17B4, ACSL1, SCD, ACSF3, PPT2, ABCD1, ACOT7, CBR4, HSD17B12, DGAT2, HACD2, ACSL5*

Supplemental Table II. RNA-Seq functional enrichment data of 5-week-old PLN-R14$^{\Delta/\Delta}$ mice hearts for terms that were identified exclusively in PLN-R14$^{\Delta/\Delta}$ mice.

Gene Ontology biological process term	Padj	NES	Leading-edge genes
GO_PROTEASOMAL_PROTEIN_CATABOLIC_PROCESS	0.0189	1.35	*CLU, SDF2L1, APOE, **DERL3**, **DERL1**, SELENOS, TREM2, RNF19B, **DNAJB9**, ARRB2, CEBPA, IL33, UCHL1, HM13, GPX1, HSP90B1, ANAPC15, RCN3, **HSPA5**, EDEM2, SEL1L, SDCBP, EDEM1, **UBE2G2**, SPSB2, DERL2, RPS27A, GBA, OS9, UBXN4, SYVN1, TRIB3, SEC61B, UGGT1, STT3B, NUPR1, ARRB1, WWP2, RACK1, RNF180, DAB2, RPL11, PSMD8, **PSMD5**, PMAIP1, **DDIT3**, MAP1A, ERLIN1, **EDEM3**, NKD2, MAEA, ZFAND2A, DNAJC10, PSMD11, UBE2W, **HSPA1B**, **HSPA1A**, WFS1, **PSMD13**, AMFR, AUP1, UBB, RNFT1, UBXN8, PSEN1, BAG2, PSMD7, UBE2J1, ARIH1, CDC16, TOR1A, FBXO17, DDA1, RHBDF1, BCAP31, UBE2D3, RHBDD1, PSMA5, PSMD14, PSMB8, SKP2, DESI1, UBE2E1, BUB1B, PSMD10, FAF2, AURKA, PLK1, CCNF, UBXN1, ANAPC10, PLAA, FBXL14, **PSMB1**, RNF121, PSMB10, RAD23B, ECRG4, PSMB9, PARK7, FBXL19, TMF1, GET4, CSNK1A1, ENC1, FBXL13, VCP, FBXL15, ANAPC7, CUL4B*
GO_REGULATION_OF_CELLULAR_AMINE_METABOLIC_PROCESS	0.0458	1.55	*ITGB2, ITGAM, NQO1, ODC1, PDE1B, SLC7A11, AZIN1, PSMD8, **PSMD5**, SLC7A7, PSMD11, **PSMD13**, PSMD7, PSMA5, PSMD14, PSMB8, PSMD10, CLN3, **PSMB1**, PSMB10, PSMB9, PARK7, NR1H4*
GO_PROTEIN_FOLDING	0.0017	2.05	*CLU, P4HB, DNAJB11, PDIA4, **DERL1**, CALR, DNAJC3, PDIA3, PDIA6, HSP90B1, PPIB, NPPA, **HSPA5**, ERP29, PRDX4, MLEC, GRN, HSPB1, QSOX1, PDIA5, CD74, LMAN1, PPIA, HSPA13, UGGT1, ERO1B, SELENOF, MOGS, SPHK1, FKBP9, CCT5, SIL1, HSP90AA1, CRTAP, P3H1, CCT3, NPPB, MESD, DNLZ, CANX, GNAO1, NUDCD2, DNAJC10, **HSPA1B**, **HSPA1A**, WFS1, TBCA, AMFR, CRYAB, GNG2, RP2, **DNAJB4**, BAG2, B2M, PRKCSH, PPIC, TOR1A, POFUT2, ERO1A, ST13, PDCL3, ERP44, PTGES3, DNAJC1, ALG12, PFDN1, CCT8, FKBP1B, UBXN1, TTC1, CCT2, RAD23B, HSPH1, GNAI3, VCP, TCP1, CHCHD4, FKBP1A, HSPA1L, DNAJC2, GNB1, CCT6A*
GO_RESPONSE_TO_TOPOLOGICALLY_INCORRECT_PROTEIN	0.0017	2.48	*CLU, DNAJB11, SDF2L1, **DERL3**, **DERL1**, CALR, SELENOS, MANF, DNAJC3, **DNAJB9**, HYOU1, SSR1, SERP1, PDIA6, CDK5RAP3, LMNA, HSP90B1, **HSPA5**, THBS4, EDEM2, HSPB1, GOSR2, GFPT1, PDIA5, EDEM1, CCL2, ASNS, DERL2, SRPRA, SERPINH1, CREB3, UBXN4, MYDGF, THBS1, XBP1, SYVN1, HSPA13, UGGT1, STT3B, **ATF4**, RACK1, KDELR3, FICD, SRPRB, PTPN1, CREB3L2, **DDIT3**, BAX, HSP90AA1, CHAC1, ATF3, HSPB8, **EDEM3**, TLN1, TM7SF3, FKBP14, CANX, UBE2W, **HSPA1B**, **HSPA1A**, WFS1, TPP1, BAK1, ARFGAP1, AMFR, AUP1, **DNAJB4**, ATP6V0D1, SEC31A, CREB3L1, HERPUD2, TSPYL2, TOR1A, COMP, MBTPS2, YIF1A, CREB3L3, ERO1A, EXTL3, ERP44, RHBDD1, HSPB2, FAF2, PACRG, TBL2, RNF121, GET3, HSPH1, ATF6B, VCP, PPP1R15A, SHC1, TMBIM6, HSPA1L, DAXX, PREB*
GO_INNATE_IMMUNE_RESPONSE_ACTIVATING_SIGNAL_TRANSDUCTION	0.0017	1.87	*FCER1G, CLEC4A, PRKCD, PAK1, CLEC4D, HCK, CLEC4C, SYK, CLEC6A, PLCG2, PAK3, MUC15, CARD9, KLRK1, RELB, PSMD8, **PSMD5**, CLEC4E, PSMD11, **PSMD13**, SRC, CARD11, CD209, PSMD7, PSMA5, PSMD14, PSMB8, PSMD10, BCL10, LYN, NRAS, **PSMB1**, PSMB10, PSMB9*
GO_TUMOR_NECROSIS_FACTOR_MEDIATED_SIGNALING_PATHWAY	0.0017	1.92	*TNFRSF11A, TNFRSF1B, SYK, TNFRSF1A, MAP3K14, OTULIN, PTK2B, TRAF3, TNFRSF11B, RACK1, EDA2R, SPHK1, TRAF1, PSMD8, **PSMD5**, TNFSF18, TNFRSF13B, TNFRSF12A, TXNDC17, TRAF2, LTBR, BIRC3, KRT18, PSMD11, **HSPA1B**, **HSPA1A**, **PSMD13**, TNFAIP3, CYLD, CASP1, CARD16, PSMD7, LTB, PLVAP, COMMD7, AIM2, TNFSF13B, PSMA5, PSMD14, ADAM17, PSMB8, TRADD, PSMD10, TNFRSF4, CLIP3, **PSMB1**, PSMB10, PSMB9, NR1H4, EDA, TRAF5, GAS6, SPPL2A, MIR27B, PSMA3, TNFSF12, PYCARD, TNF, TNFSF9*
GO_LUNG_MORPHOGENESIS	0.0370	1.64	*CTSZ, TNC, CTSH, CDC42, TGFBR2, PLOD3, SOX9, STK40, LIF, MAP2K1, FOXP2*
GO_INORGANIC_ION_IMPORT_ACROSS_PLASMA_MEMBRANE	0.0158	-1.66	*WNK2, HCN2, ABCC9, ATP1B2, RAMP3, SLC12A2, TRPM4, KCNJ8, KCNJ2, ATP2B4, KCNJ11, FYN, WNK4, SLC5A1, SLC12A5, CACNA2D1, ISCU, SLC12A7, KCNJ3, ATP1A2, ATP1A1*
GO_FATTY_ACYL_COA_METABOLIC_PROCESS	0.0220	-1.76	*ACSL1, GCDH, HSD17B4, ACOT7, ACAT1, TECR, DGAT2, ACSF3, CBR4, ACSL6, ELOVL5*

Supplemental Table III. RNA-Seq functional enrichment data of 8-week-old PLN-R14$^{\Delta/\Delta}$ mice hearts for terms that were identified exclusively in PLN-R14$^{\Delta/\Delta}$ mice.

Gene Ontology biological process term	Padj	NES	Leading-edge genes
GO_PROTEASOMAL_PROTEIN_CATABOLIC_PROCESS	0.0024	1.61	***UBE2G2***, *UCHL1, APOE, NUPR1, PSMD8, CLU, OS9, GBA, GPX1, RPS27A, RPL11, RNF19B, UBXN4, RACK1, SELENOS,* ***DERL3****, KCTD10, TREM2, MAP1A, UBB, DNAJC10, MAEA, SDCBP, PSMC1, ZFAND2A, PSMA5, GCLC, HFE, EDEM2, GET4, ENC1, SPSB2, PSMD11, UBXN1, PSMC4, PKD1, UBE2J1,* ***PSMD13****, RNF103,* ***PSMB1****, RCN3, WWTR1, TRIB3,* ***DERL1****, PLK2, WWP2, FBXO17, HM13, TOR1A, SDF2L1, STT3B, CEBPA, UFD1, DDA1, NKD2, ECRG4,* ***PSMD5****, SEL1L, ARRB2, EDEM1, RNF144B, IL33,* ***PSMA2****, CUL4B, DDB1,* ***DNAJB9****, RCHY1, FBXW8, FAM122A, ANAPC15, NPLOC4, NHLRC3, UBXN8, PSMA3, RHBDF1, FBXO9, ARRB1, PPP2CB, PSMD14, FBXL3, CSNK1A1, HSP90B1, ANAPC4, RNF19A, PELI1, RNFT1, SIAH1, PSMD4, SIRT2, PSMA6, AUP1, ANAPC2, TRIM3, ARIH2, TBL1X, FBXL4, PMAIP1,* ***DDIT3****, BAG5, SMAD7, TRIM2, FOXRED2, TAF9, PSMA7, NOP53, ECSCR,* ***HSPA5****, PLAA, ARIH1, SEC61B, GIPC1, ERLEC1, RNF4, AMFR, HECW2, SGTB, AMN1, BCAP31, NUB1, PCBP2, PIAS1, PSMB4, RNF185, PSMD7, FMR1, TLK2, CD2AP, PSMB3, PSMF1, TBL1XR1, GABARAPL2*
GO_REGULATION_OF_CELLULAR_AMINE_METABOLIC_PROCESS	0.0140	1.67	*PSMD8, ITGB2, PSMC1, PDE1B, PSMA5, ITGAM, PSMD11, PSMC4, NQO1,* ***PSMD13****,* ***PSMB1****,* ***PSMD5****,* ***PSMA2****, COMT, PSMA3, SLC7A11, PSMD14, ABAT, PSMD4, PSMA6, PSMA7, PSMB4, PSMD7, PSMB3, PSMF1, PSMC6*
GO_PROTEIN_FOLDING	0.0155	1.50	*SPHK1, SELENOF, P4HB, CLU, GRN, PPIB, QSOX1, PPIA, FKBP5, PPIC, FKBP9, PRDX4, GNAO1, DNAJC10, GNG2, PSMC1, DNAJC3, CRTAP, GNAI2, DNAJB11, TBCD, NPPA, TBCA, UBXN1, PDIA3, PFDN5, PDCL3,* ***DERL1****, GNB1, TOR1A, HSPB1, GNAI3, PDIA4, TTC1, HSP90B1, NPPB, GAK, FKBP1B, P3H1, BAG5, SIL1,* ***HSPA5****, LTBP4, FUT10, PPIG, FKBP1A, ERP29, GNAI1, PRKCSH, CCT8, TBCE, AMFR, SGTB, ERO1A, CALR, DNAJB6, GNB2, HSPA13, PFDN1, PDIA5, PDIA6,* ***DNAJB4****, WFS1, CCT5, NUDCD2, FKBP8, DNAJC2, MPDU1, CCT3, B2M*
GO_RESPONSE_TO_TOPOLOGICALLY_INCORRECT_PROTEIN	0.0030	1.70	*COMP, CLU, CREB3, LMNA, UBXN4, RACK1, THBS4, SELENOS,* ***DERL3****, SHC1, SERP1, DNAJC3, BOK, DNAJB11, EDEM2,* ***ATF4****, TSPYL2, ATP6V0D1, CDK5RAP3, ASNS, PPP1R15A, DAXX,* ***DERL1****, TM7SF3, SSR1, TOR1A, HSPB1, PTPN1, SDF2L1, STT3B, UFD1, EDEM1, THBS1,* ***DNAJB9****, GOSR2, CTDSP2, SULT1A3, SULT1A4, HSPB7, KDELR3, STC2, HSP90B1, CREB3L2, BAX, AUP1, PTPN2, TATDN2, XBP1,* ***DDIT3****, SEC31A,* ***HSPA5****, TLN1, FKBP14, MYDGF, AMFR, COPS5, EIF2AK3, RNF185, ERO1A, CREB3L4, CALR, HERPUD2, ARFGAP1, HSPA13, PDIA5, MANF, PDIA6,* ***DNAJB4****, WFS1, FAF2, DERL2*
GO_INNATE_IMMUNE_RESPONSE_ACTIVATING_SIGNAL_TRANSDUCTION	0.0066	1.70	*PSMD8, FCER1G, CLEC4D, PRKCD, PAK3, CLEC4A, PSMC1, PSMA5, PSMD11, PSMC4,* ***PSMD13****, PAK1,* ***PSMB1****, CLEC6A,* ***PSMD5****,* ***PSMA2****, CLEC4C, PLCG2, MUC15, PSMA3, PSMD14, BCL10, PSMD4, PSMA6, CLEC4E, PSMA7, SRC, HCK, PSMB4, PSMD7, MUC1, PSMB3, PSMF1, SYK, PSMC6*
GO_TUMOR_NECROSIS_FACTOR_MEDIATED_SIGNALING_PATHWAY	0.0030	1.77	*GAS6, SPHK1, PSMD8, TNFRSF1A, PLVAP, OTULIN, RACK1, PTK2B, TXNDC17, NFKBIA, PSMC1, CLIP3, LTBR, PSMA5, PSMD11, PSMC4,* ***PSMD13****,* ***PSMB1****, TNFRSF1B, HIPK1, BIRC3, TAX1BP1,* ***PSMD5****,* ***PSMA2****, TNFRSF11A, FAS, PSMA3, ACTN4, EDA, PSMD14, KRT18, PSMD4, PSMA6, PTPN2, TNFRSF12A, TNFSF13B, PSMA7, CYLD, MIR27B, PSMB4, PSMD7, TNFRSF13B, PSMB3, PSMF1, KRT8, TNFSF12, SYK, TNFSF18, PSMC6, BIRC2, TRAF1, AIM2, TNFRSF11B, ILK, NR1H4, MAP3K14*
GO_LUNG_MORPHOGENESIS	0.0171	1.73	*SPRY1, CTSZ, TGFBR2, CTSH, BMP4, FGFR2, CDC42, DLG5, TCF21, FOXP2, MAPK3, AP3B1, TNC, PLOD3, FOXF1, MAP2K1, FGF7, SEC24B*
GO_INORGANIC_ION_IMPORT_ACROSS_PLASMA_MEMBRANE	0.0250	-1.65	*ABCC9, ATP1A2, ATP1B2, HCN2, SLC9A2, KCNJ5, TRPM4, CNGA3, KCNJ2, WNK2, KCNJ3, KCNJ8, SLC12A7*
GO_FATTY_ACYL_COA_METABOLIC_PROCESS	0.0092	-1.84	*DGAT2, ACSL1, TECR, GCDH, ACAT1, HSD17B4, CBR4, ACOT7, ABCD1, ACSL6, ACSF3*

Supplemental Table IV. RNA-Seq functional enrichment data of mice hearts 3 days post-I/R for terms that were identified exclusively in PLN-R14$^{\Delta/\Delta}$ mice.

Gene Ontology biological process term	Padj	NES	Leading-edge genes
GO_PROTEASOMAL_PROTEIN_CATABOLIC_PROCESS	0.9258	-0.92	*NFE2L1, GNA12, GID4, ALAD, PSME4, SVIP, CCDC47, FBXW7, PRICKLE1, PRPF19, ECPAS, UBR3, FBXW5, KEAP1, SKP1, PRKACA, USP13, RMND5A, DCAF11, UBE2B, CUL3, DMAC2, ZER1, UBR2, USP19, PINK1, CUL4A, WFS1, PSMD12, BFAR, PPP2R5C, CUL5, CLEC16A, VCP, CUL2, SCO1, CUL1, AREL1, RNF14, DET1, UBE2H, UBQLN4, FBXO9, PSMD1, GSK3A, BAG6, RNF144A, HUWE1, MARCHF6, PSMB7, SH3RF2, FBXO22, USP14, HERC2, TRIB2, ZNRF1, ARMC8, PSMC6, FBXO31, BTRC, FAM122A, SGTA, MAPK9, COP1, ARAF, NPLOC4, UBXN2A, CRBN, UGGT2, DNAAF4, RNF216, CDC23, UFD1, TLK2, ZYG11B, FBXO6, PLAA, HSP90AB1, UBXN6, ANAPC4, NEDD4L, NR1D1, PRKN, PSMC2, PSMF1, PSME1, FBXL3, UBE2D1, GID8, TMEM129, DNAJB2, PSMC3, TRIM72, CTNNB1, HECTD3, PSMD7, PSMD2, UFL1, DNAJC18, RNF139, KLHL40, FAF1, CDC34, PARK7, FBXL12, MTM1*
GO_REGULATION_OF_CELLULAR_AMINE_METABOLIC_PROCESS	0.6026	1.01	*ITGB2, ITGAM, SLC7A7, CLN3, PDE1B, SLC7A11, ODC1, AZIN1, PSMB8*
GO_PROTEIN_FOLDING	0.3352	1.14	*GRN, P3H1, GNB1, PPIB, PPIA, P4HB, PDIA3, CRTAP, ERP29, GNG2, PDIA5, PRDX4, PPIC, GNAI2, SPHK1, PDIA6, GNB2, DNAJB11, PDIA4, GNAI3, SELENOF, GANAB, CLU, CALR, TOR2A, UGGT1, FKBP1A, QSOX1, UNC45A, TOR1A, DNAJC10, NUDCD2, MPDU1, DNAJC3, MOGS, ERO1B, HSP90B1, FKBP1B, GAK, FKBP5, POFUT2, FUT10, SNRNP70, NKTR, RP2, CCT5, CSNK2A2, BAG5, NPPA, CCT2*
GO_RESPONSE_TO_TOPOLOGICALLY_INCORRECT_PROTEIN	0.2881	1.17	*SERP1, EDEM1, PTPN1, CREB3L1, SERPINH1, SSR1, KDELR3, PDIA5, PDIA6, DNAJB11, SDF2L1, CCL2, RACK1, LMNA, PTPN2, CLU, CALR, BOK, MYDGF, ATP6V0D1, BAX, THBS1, ARFGAP1, BAK1, UGGT1, PPP1R15B, ATF3, TOR1A, MANF, TLN1, FKBP14, DAXX, DNAJC3, EDEM2, DDX11, SHC1, CREB3L3, CREB3L2, AUP1, XBP1, HSP90B1, CREB3, EIF2AK2, EIF2AK3, TBL2, ASNS, SRPRB*
GO_INNATE_IMMUNE_RESPONSE_ACTIVATING_SIGNAL_TRANSDUCTION	0.0743	1.41	*FCER1G, CLEC4D, CLEC6A, HCK, CLEC4C, LYN, PRKCD, CLEC4A, CARD9, NRAS, PAK1, SYK, CARD11, RELA, CLEC4E, MUC15, PSMB8, BCL10, SRC, KLRK1, PAK2, PAK3, CD209, PLCG2, RELB*
GO_TUMOR_NECROSIS_FACTOR_MEDIATED_SIGNALING_PATHWAY	0.0598	1.39	*TNFRSF1B, TNFRSF11A, TNFRSF1A, PLVAP, RIPK1, LTBR, CASP8, SPHK1, TRAF1, SYK, RELA, RACK1, CD40, PTPN2, ACTN4, TNFRSF13B, AIM2, PSMB8, BIRC3, ILK, TRAIP, CASP1, CARD16, PTK2B, JAK2, CARD14, CPNE1, TP53, TNFSF12, TNFRSF12A, ADAM17, NFKBIA, TXNDC17, TRAF5, GAS6, PYCARD, IKBKB, CLIP3*
GO_LUNG_MORPHOGENESIS	0.1178	1.42	*TNC, CTSZ, CTSH, PLOD3, CDC42, LIF, TGFBR2, RDH10, SOX9, ID1, MAPK3, FOXP2, SRSF6, SPRY2, KRAS, HOXA5, FOXF1, SPRY1, VANGL2, SEC24B*
GO_INORGANIC_ION_IMPORT_ACROSS_PLASMA_MEMBRANE	0.1871	-1.26	*KCNJ2, KCNJ5, ATP1A2, TRPM4, SLC12A7, KCNJ11, KCNJ3, CNGA3, ISCU, WNK2, CACNA2D1, KCNJ8, WNK1, KCNH2, ABCC9, HCN4, DLG1, SLC9A6, SLC12A5, SLC24A2*
GO_FATTY_ACYL_COA_METABOLIC_PROCESS	0.2391	-1.28	*HSD17B4, ACSL1, ACAT1, ACSF3, TECR, CBR4, GCDH*

Supplemental Table V. RNA-Seq functional enrichment data of mice hearts 8 weeks post-MI for terms that were identified exclusively in PLN-R14$^{\Delta/\Delta}$ mice.

Gene Ontology biological process term	Padj	NES	Leading-edge genes
GO_PROTEASOMAL_PROTEIN_CATABOLIC_PROCESS	1.0000	0.72	*UCHL1, NKD2, NUPR1, RCN3, PKD1, ECRG4, KCTD17, MAP1A, GPX1, SPSB4, ARRB1, AKT1, SPSB2, DAB2, KCTD10, FBXO17, UBXN11, FBXL14, UBE2C, SUMO2, RHBDF1, FBXL2, WWTR1, RMND5B, SMURF2, PML, CLU, UBXN4, PSMC4, MAEA, CDC20, BCAP31, PSMD14, DNAJC10, PMAIP1, RHBDD1, TRIM72, PBK, APOE, SDCBP, CLEC16A, AURKB, GIPC1, OS9, CDK1, HFE, SIRT6, ECSCR, SMAD7, DESI1, WWP2, KCTD5, ZFAND2A, FBXL22, CSNK1D, CEBPA, AURKA, RNF41, TREM2, BAG2, ARIH1, PSMB10, TAF9, FBXL16, RNF4, SPSB3, CCNB1,* ***UBE2G2****, JKAMP, HSPBP1, PSMD8, TMF1, DDA1, ANAPC7, EDEM1, CCNF, PSMA5, TRIM2, RNF34, SMURF1, FBXW11, ANAPC15, UFD1, GLMN, PSMA3, MAD2L1, PSMD11, CHFR, HSP90AB1, UGGT1, FBXL8, UBE2J1, CDC27, XPO1, ARRB2, BAG5*
GO_REGULATION_OF_CELLULAR_AMINE_METABOLIC_PROCESS	0.7666	0.90	*AZIN1, ODC1, ITGAM, SLC7A7, ITGB2, COMT, PSMC4, PSMD14, PDE1B, ABAT, PSMB10, PSMD8, PSMA5, PSMA3, PSMD11*
GO_PROTEIN_FOLDING	0.3659	1.12	*LTBP4, NPPA, GNAO1, GNB1, SELENOF, GNAI2, QSOX1, HSP90AA1, POFUT2, PPIC, PPIB, CLU, CRTAP, CCT3, NPPB, GRN, MLEC, DNAJC10, RIC3, HSPH1, FKBP1A, GANAB, HSPA4L, GNB4, CCT8, DNAJB6, HSPA1L, PRKCSH, HSPB1, BAG2, MPDU1, FKBP1B, PDIA3, DFFA, PPIA, DNAJC3, UNC45A, GNG2, SPHK1, FKBP9, B2M, HSPBP1, AHSA1, P3H1, PRDX4, P4HB, DNAJC2, HSPB6, HSP90AB1, UGGT1, GNB2, FUT10, CALR, BAG5, PDIA4, HSPA13, PPID, AMFR, ERO1A, DNAJB11, VCP, MOGS, TBCEL, HSPA8, CHORDC1, DNAJC5, TBCC*
GO_RESPONSE_TO_TOPOLOGICALLY_INCORRECT_PROTEIN	0.2568	1.18	*COMP, CREB3L2, THBS4, TLN1, LMNA, PTPN2, HSP90AA1, SERPINH1, BOK, CLU, UBXN4, PTPN1, HSPA4, SHC1, BAK1, HSPB3, THBS1, RHBDD1, WIPI1, MBTPS1, HSPH1, SEC31A, TM7SF3, CREB3L1, HSPA4L, SSR1, CCND1, CREB3L3, KDELR3, MYDGF, HSPA1L, ATF6B, BAX, HSPB1, HSPB8, CREB3, DNAJC3, HSPB7, FKBP14, MBTPS2, JKAMP, EIF2AK2, EDEM1, SERP1, UFD1, HSP90AB1, UGGT1, HSF1, TMEM33, DDX11, HDAC6, CALR, HSPA13, TATDN2, DAXX, AMFR, ERO1A, DNAJB11, RNF121, VCP, ARFGAP1, HDGF*
GO_INNATE_IMMUNE_RESPONSE_ACTIVATING_SIGNAL_TRANSDUCTION	0.7069	0.95	*PLCG2, CARD11, FCER1G, PAK3, RELA, PSMC4, PRKCD, MUC15, PSMD14, SYK, RELB, MUC1, CLEC6A, KRAS, PSMB10, PAK1, CLEC4D, PSMD8, PSMA5, HCK, SRC, CD209, FBXW11, FYN, NFKB1, PSMA3, PSMD11*
GO_TUMOR_NECROSIS_FACTOR_MEDIATED_SIGNALING_PATHWAY	0.1850	1.25	*ADIPOQ, PLVAP, TRAF3, ACTN4, PTPN2, TNFRSF11B, TNFRSF1A, TNFRSF12A, TRAF1, GAS6, PTK2B, TNFRSF1B, F2RL1, CLIP3, RELA, PSMC4, OTULIN, PSMD14, TP53, TNFSF12, SYK, CASP8, APOA1, EDA, BIRC3, TNFRSF11A, RIPK1, LTBR, CYLD, PSMB10, SPHK1, MIR27B, CD40, TNFSF18, PSMD8, PSMA5, TNFAIP3, ADAM17, PSMA3, PSMD11, TRADD, CASP1, CARD16*
GO_LUNG_MORPHOGENESIS	0.0926	1.48	*CTSZ, TGFBR2, PLOD3, TNC, DLG5, FOXP2, TCF21, SOX9, HOXA5, FGFR2, CDC42, KRAS, STK40, SRF, SPRY1, NOG, BMP4, LIF, VANGL2, MAPK3, FGF7, MAP2K1*
GO_INORGANIC_ION_IMPORT_ACROSS_PLASMA_MEMBRANE	0.7323	-0.92	*KCNJ5, ATP1A2, SLC9A2, ABCC9, TRPM4, CNGA3, SLC5A1, SLC9A6, CACNA2D1, KCNJ2, WNK2, KCNJ8, KCNJ3*
GO_FATTY_ACYL_COA_METABOLIC_PROCESS	0.4557	-1.11	*ACOT7, GCDH, DGAT2, ACAT1, ACSL6, HSD17B8, ACSL1, ACSBG1, PPT1, ACSL3, ABCD1, TECR, CBR4, ACSF3, HSD17B4, PPT2*

Supplemental Table VI can be downloaded as a separate supplemental file.

Supplemental Table VII. LC-MS/MS enrichment data of the significantly enriched GO terms in downregulated proteins in 3-week-old PLN-R14$^{\Delta/\Delta}$ mice hearts.

Gene Ontology biological process term	Padj	Gene symbols
Translation	4.71E-14	*Rps3a, Kars1, Rps7, Eif4g1, Rps18, Rpl27a, Rps17, Rps16, Farsb, Eef2, Rpl19, Rpl35, Gfm2, Rpl32, Rpl31, Rpl13, Mrps15, Rps20, Rps13, Eif4a1, Rps15*
Protein folding	0.0030	*Cct4, Cryab, Cct7, Fkbp4, Dnaja2, Pdia4, Tcp1*
Metabolic process	0.0030	*Ephx2, Gsta4, Pygm, Prdx6, Pygb, Pgam1, Acss1, Gsto1, Pfkp, Pfkm, Cndp2*
Ribosomal small subunit biogenesis	0.0075	*Rps17, Rps16, Rps7, Rps15*
Positive regulation of protein localization to Cajal body	0.0446	*Cct4, Cct7, Tcp1*
Positive regulation of establishment of protein localization to telomere	0.0477	*Cct4, Cct7, Tcp1*

Supplemental Table VIII. LC-MS/MS enrichment data of the 30 most significantly enriched GO terms in upregulated proteins in 5-week-old PLN-R14$^{\Delta/\Delta}$ mice hearts.

Gene Ontology biological process term	Padj	Gene symbols
Translation	1.03E-39	*Rpl8, Rps5, Rpl11, Rpl12, Rpl18a, Rpl13a, Eef1b, Rps11, Dars1, Rpl7a, Rpl27a, Rpl29, Rpl23a, Rpl18, Rpl21, Rpl32, Rps2, Rpl6, Eef1a2, Rps6, Rps3a, Rpl14, Rps24, Rpl34, Eef1a1, Eif4g1, Rpl17, Eef1d, Rps8, Rpl35a, Rps15a, Rpl19, Rpl36a, Rpl27, Eif3a, Eif3e, Rps20, Rpl15, Rpl10a, Wars1, Rpl10, Rpl37, Rack1, Eprs1, Rps3, Rpl9, Vars1, Rps19, Eef1g, Eif3i, Eif3c, Rps18, Rpl7, Rps17, Rps9, Rps23, Eef2, Rpl26, Rpl4, Rpl5, Rpl13, Rpl31, Rpl24, Rpl3, Rps27a, Rpl28, Eif4a1*
Protein folding	2.78E-12	*Pdia3, Cct4, Cct2, Cct7, Hsp90aa1, Tubb5, St13, Tcp1, Hsp90ab1, Canx, Ppia, Cryab, Calr, Cct8, Hsp90b1, Pdia4, P4hb, Txnl1, Pdia6, Cct3, Hspa8, Cct6a, Cct5*
Positive regulation of protein localization to Cajal body	3.95E-09	*Cct4, Cct2, Cct7, Cct8, Tcp1, Cct3, Cct6a, Cct5*
Cytoplasmic translation	2.08E-07	*Rpl8, Rpl29, Rpl35a, Rpl9, Rplp2, Rpl26, Rplp0, Rpl31, Rpl6, Rpl7, Rpl15*
Antigen processing and presentation of exogenous peptide antigen via MHC class I, TAP-dependent	9.27E-07	*Calr, Psma3, Psmb4, Psma4, B2m, Psma5, Psma6, Psma1, Psmb2, Psma7*
Cell-cell adhesion	9.27E-07	*Pdlim1, Rpl14, Vapa, Eef1g, Ehd4, Eif4g1, Hdlbp, Eef1d, Rpl7a, Plec, Lasp1, Ywhaz, Eno1, Septin2, Rps2, Pfkp, Eif3e, Tagln2, Tln1, Rpl15*
Positive regulation of establishment of protein localization to telomere	9.27E-07	*Cct4, Cct2, Cct7, Cct8, Tcp1, Cct6a, Cct5*
Positive regulation of telomerase RNA localization to Cajal body	1.06E-06	*Cct4, Cct2, Cct7, Cct8, Tcp1, Cct3, Cct6a, Cct5*
Toxin transport	2.62E-06	*Cct4, Cct2, Cct7, Cct8, Hspa5, Tcp1, Copb2, Cct3, Cct6a, Cct5*
Proteolysis involved in cellular protein catabolic process	1.79E-05	*Psma3, Hspa5, Psmb4, Ide, Psma4, Plg, Psma5, Psma6, Psma1, Psmb2, Psma7*
Positive regulation of telomere maintenance via telomerase	1.79E-05	*Cct4, Cct2, Cct7, Cct8, Ctnnb1, Tcp1, Cct3, Cct6a, Cct5*
Vesicle-mediated transport	2.03E-05	*Gdi2, Rab2a, Copg1, Bcap31, Cltc, Ap2b1, Ap2a1, Sar1a, Sec31a, Copa, Clta, Copb2, Ap1g1, Lman1, Cltb, Arcn1, Tmed10, Arf3, Rab1A*
Binding of sperm to zona pellucida	4.09E-05	*Cct4, Cct2, Cct7, Cct8, Tcp1, Cct3, Cct6a, Ubap2l, Cct5*
Ribosomal large subunit assembly	5.19E-05	*Rpl11, Rpl12, Rpl23a, Rpl10, Rpl5, Rpl24, Rpl3, Rpl6*
Protein stabilization	1.17E-04	*Cct4, Cct2, Cct7, Flot2, Flna, Tcp1, Clu, Calr, Cct8, Npm1, Cct3, Pfn1, Cct6a, Cct5*
Positive regulation of RNA polymerase II transcriptional preinitiation complex assembly	1.93E-04	*Psmc4, Psmc2, Psmc5, Psmc1, Psmc3, Psmc6*
Intracellular protein transport	2.36E-04	*Rab2a, Copg1, Bcap31, Ran, Cltc, Ap2b1, Kpnb1, Ap2a1, Sar1a, Copa, Ywhah, Clta, Copb2, Ap1g1, M6pr, Cltb, Tmed10, Rab1A*
Ribosomal large subunit biogenesis	4.54E-04	*Rpl11, Rpl35a, Rpl14, Rpl26, Rpl5, Npm1, Rpl7*
Platelet degranulation	8.06E-04	*Calu, Cap1, Hspa5, Cfl1, Pfn1*
ER-associated ubiquitin-dependent protein catabolic process	0.0010	*Vcp, Psmc4, Ecpas, Psmc2, Psmc5, Hsp90b1, Psmc1, Psmc3, Psmc6*
Protein transport	0.0021	*Copg1, Gdi2, Bcap31, Pdcd6ip, Snx3, Kpnb1, Ap2a1, Copa, Tmed9, Lman1, Ap1g1, Tmed10, Arf3, Rab2a, S100a13, Ran, Ap2b1, Ccdc93, Scamp2, Sar1a, Sec31a, Actn4, Tmed4, Rab14, Copb2, Arcn1, Rab35, Rab1A*
Protein catabolic process	0.0022	*Psmc4, Psmc2, Psmc5, Ctsd, Psmc1, Psmc3, Psmc6, Cast*
Small GTPase mediated signal transduction	0.0037	*Gdi2, Rhoc, Rab2a, Rras, Ran, Rac1, Rap1b, Rhoa, Ralb, Rab14, Srprb, Cdc42, Rab35, Arf3, Gna12, Rab1A*
Cellular response to interleukin-4	0.0100	*Mrc1, Hspa5, Rplp0, Hsp90ab1, Rpl3, Rps2*
Establishment or maintenance of cell polarity	0.0100	*Cap1, Ctnna1, Actr2, Cap2, Cdc42, Actr3*
rRNA processing	0.0101	*Rps17, Rpl11, Rpl35a, Rpl14, Rps19, Rpl26, Rps24, Pa2g4, Rpl5, Rpl7, Rps6*
Ubiquitin-dependent protein catabolic process	0.0117	*Vcp, Psma3, Psmd4, Psmc2, Psma4, Psmd11, Psma5, Psma6, Psma1, Psmd13, Psmd3, Psma7*
Arp2/3 complex-mediated actin nucleation	0.0126	*Actr2, Arpc2, Arpc3, Arpc4, Actr3*
Translational elongation	0.0156	*Rplp2, Eef2, Eef1g, Eef1a1, Eef1b, Eef1d, Eef1a2*
Positive regulation of substrate adhesion-dependent cell spreading	0.0215	*Rac1, Calr, S100a10, Arpc2, Flna, Cdc42*

Supplemental Table IX. LC-MS/MS enrichment data of the 30 most significantly enriched GO terms in upregulated proteins in 8-week-old PLN-R14$^{\Delta/\Delta}$ mice hearts.

Gene Ontology biological process term	Padj	Gene symbols
Translation	8.34E-29	*Rpl8, Rps5, Rpl11, Rpl12, Rpl18a, Rpl13a, Eef1b, Rps11, Dars1, Rpl7a, Rpl27a, Rpl29, Rpl23a, Rps12, Rpl18, Rpl21, Eif3l, Rps2, Rpl6, Rps6, Rpl14, Rps24, Rpl34, Eef1a1, Rpsa, Rpl17, Eef1d, Rps8, Rpl35a, Rps15a, Rpl19, Rpl36a, Rpl27, Eif3a, Rpl30, Eif3e, Rpl15, Rpl10a, Wars1, Rpl10, Rpl37, Rack1, Eprs1, Gars1, Gfm2, Rps3, Rpl9, Vars1, Rps19, Eef1g, Eif3i, Eif3c, Rpl7, Rps21, Rps9, Rps23, Farsb, Rpl26, Rpl4, Rpl5, Rpl13, Rpl24, Rpl3, Rps27a, Rpl36, Eif4a1*
Protein folding	6.69E-11	*Pdia3, Txn, Hsp90aa1, Tubb5, St13, Tcp1, Cryab, Pdia4, Pdia6, Cct4, Cct2, Cct7, Canx, Ppia, Calr, Cct8, Pfdn1, Hsp90b1, P4hb, Tmx1, Txnl1, Cct3, Hspa8, Cct6a, Cct5*
Proteolysis involved in cellular protein catabolic process	6.69E-11	*Ctsb, Psma3, Psmb4, Psmb7, Psma4, Capn2, Plg, Psma1, Psmb2, Psmb6, Hspa5, Ide, Psmb5, Psma5, Psma6, Psmb1, Psma7, Lonp1*
Antigen processing and presentation of exogenous peptide antigen via MHC class I, TAP-dependent	1.62E-10	*Psma3, Psmb4, Psmb7, Psma4, Psma1, Psmb2, Psmb6, Calr, Psmb5, B2m, Psma5, Psma6, Psmb1, Psma7*
Cell-cell adhesion	4.32E-09	*Vapa, Lasp1, Rpl7a, Fscn1, Ywhaz, H3c1; H3c8; H3c10; H3c11, Rab10, Septin2, Bag3, Rps2, Tln1, Pdlim1, Rpl14, Ywhab, Pdlim5, Eef1g, Ehd4, Hdlbp, Eef1d, Psmb6, Plec, Ldha, Eno1, Eif3e, Pfkp, Tagln2, Rpl15*
Positive regulation of protein localization to Cajal body	3.12E-08	*Cct4, Cct2, Cct7, Cct8, Tcp1, Cct3, Cct6a, Cct5*
Cytoplasmic translation	2.76E-07	*Rpl8, Rpl29, Rpl35a, Rpl9, Rplp2, Rpl26, Rplp0, Rpl6, Rpl7, Rplp1, Rpl36, Rpl15*
Sarcomere organization	1.49E-06	*Actn2, Prkar1a, Mybpc3, Cfl2, Itgb1, Myh6, Tpm1, Xirp1, Tnnt2, Wdr1, Ttn*
Positive regulation of establishment of protein localization to telomere	7.82E-06	*Cct4, Cct2, Cct7, Cct8, Tcp1, Cct6a, Cct5*
Positive regulation of telomerase RNA localization to Cajal body	1.28E-05	*Cct4, Cct2, Cct7, Cct8, Tcp1, Cct3, Cct6a, Cct5*
Muscle contraction	1.55E-05	*Actn2, Slmap, Mybpc3, Dysf, Anxa1, Myh6, Myl6, Acta2, Anxa2, Tnnt2, Ttn, Myom1*
Positive regulation of telomere maintenance via telomerase	2.27E-05	*Cct4, Cct2, Cct7, Cct8, Hnrnpa1, Ctnnb1, Tcp1, Cct3, Cct6a, Cct5*
Toxin transport	4.92E-05	*Cct4, Cct2, Cct7, Cct8, Hspa5, Tcp1, Copb2, Cct3, Cct6a, Cct5*
Protein stabilization	6.15E-05	*Cct4, Cct2, Cct7, Flot2, Flna, Gapdh, Tcp1, Clu, Calr, Cct8, Npm1, Pfn2, Bag3, Cct3, Pfn1, Cct6a, Cct5*
Small GTPase mediated signal transduction	7.30E-05	*Hras, Gdi1, Gdi2, Rhoc, Rab2a, Rras, Rab7a, Ran, Rab5c, Rac1, Rap1b, Rab11b, Rala, Rhoa, Ralb, Rab14, Rab10, Srprb, Cdc42, Rab35, Arf3, Gna12, Rab1A*
Cardiac muscle contraction	7.30E-05	*Mybpc3, Camk2d, Myh6, Tpm1, Tnni3, Srsf1, Myl3, Tnnc1, Tnnt2, Ttn, Slc8a1*
Intracellular protein transport	1.87E-04	*Rab2a, Copg1, Bcap31, Rab7a, Ran, Cltc, Ap2b1, Kpnb1, Ap2a1, Sar1a, Vps29, Copa, Ywhah, Clta, Scamp3, Rab10, Copb2, Ap1g1, M6pr, Cltb, Tmed10, Rab1A*
Vesicle-mediated transport	1.87E-04	*Gdi2, Rab2a, Copg1, Bcap31, Mia3, Cltc, Ap2b1, Ap2a1, Sar1a, Sec31a, Copa, Clta, Rab10, Copb2, Ap1g1, Lman1, Cltb, Arcn1, Tmed10, Arf3, Rab1A*
Protein catabolic process	4.87E-04	*Psmc4, Cul2, Psmc2, Psmc5, Ctsd, Psmc1, Psmc3, Psmc6, Cast, Lonp1*
Ribosomal large subunit assembly	5.04E-04	*Rpl11, Rpl12, Rpl23a, Rpl10, Rpl5, Rpl24, Rpl3, Rpl6*
Positive regulation of RNA polymerase II transcriptional preinitiation complex assembly	0.0011	*Psmc4, Psmc2, Psmc5, Psmc1, Psmc3, Psmc6*
Protein transport	0.0032	*Copg1, Gdi1, Gdi2, Bcap31, Pdcd6ip, Snx3, Rab5c, Kpnb1, Ap2a1, Copa, Tmed9, Scamp3, Rab10, Lman1, Ap1g1, Tmed10, Arf3, Rab2a, S100a13, Rab7a, Ran, Mia3, Ap2b1, Scamp2, Sar1a, Sec31a, Vps29, Rab11b, Actn4, Tmed4, Rab14, Copb2, Arcn1, Rab35, Rab1A*
Actin cytoskeleton organization	0.0032	*Ran, Flna, Xirp1, Fscn1, Cap1, Rac1, Rhoa, Actr2, Pfdn1, Pfn2, Tmsb4x, Pafah1b1, Wdr1, Pfn1, Epb41l2*
Ribosomal large subunit biogenesis	0.0032	*Rpl11, Rpl35a, Rpl14, Rpl26, Rpl5, Npm1, Rpl7*
Platelet degranulation	0.0032	*Calu, Cap1, Hspa5, Cfl1, Pfn1*
Glycolytic process	0.0038	*Hk1, Pfkl, Gpi, Pgam1, Gapdh, Pkm, Eno1, Pfkp*
Binding of sperm to zona pellucida	0.0038	*Cct4, Cct2, Cct7, Cct8, Tcp1, Cct3, Cct6a, Cct5*
Chaperone-mediated protein complex assembly	0.0049	*Cct2, Hsp90aa1, Hspa4, Clu, Lonp1*
Apical junction assembly	0.0049	*Rhoc, Ctnna1, Rhoa, Vcl, Wdr1*
Substantia nigra development	0.0049	*Hspa5, S100a1, Ywhah, Calm1, Cox6b1, Ywhae, Cdc42, Actb*